

1 **Optimization of irrigation scheduling for barley crop, combining**
2 **AquaCrop and MOPECO models to simulate various water-deficit**
3 **regimes**

4 Martínez-Romero, A., López-Urrea, R., Montoya, F., Pardo, J.J., Domínguez, A.*

5
6 **Abstract**

7 To optimize the irrigation scheduling of field crops to maximize irrigation water
8 productivity requires expert knowledge of the crop development and its productive
9 response to water deficit. Implementing this idea with commodities such as barley, whose
10 current global profitability is low, and, more specifically, in areas where the availability
11 of water resources for irrigation is limited, requires a proper decision support system. In
12 this research, AquaCrop and MOPECO models were used to compute and compare both
13 the crop-water production and irrigation water productivity functions generated by
14 several irrigation strategies provided by each model for the typical irrigated crop barley
15 grown in the area. Furthermore, we evaluated both models' performance with a 3-year
16 field experiment applying the methodology of optimized regulated deficit irrigation for
17 limited volumes of irrigation water (ORDIL) in barley crop. The results obtained from
18 the production functions show that gross irrigation water depths (GIWD) of more than
19 310 mm can be useful to attain the potential crop yield, depending on the criteria
20 considered to generate the irrigation scheduling. However, with less GIWD available, the
21 simulated barley development was subjected to water deficit, leading to a reduction in
22 both crop yield and irrigation water productivity, where MOPECO simulated higher crop
23 yields and irrigation water productivity values than those obtained by AquaCrop (between
24 16% and 27% and between 8.0% and 27.5% respectively) under similar GIWD levels.
25 These differences are mainly due to how the irrigation strategies are outlined in the two
26 models and the different evapotranspiration methodologies they deploy. Finally, both
27 models provided performed appropriately in simulating final crop yield (errors lower than
28 $0.50 \times 10^3 \text{ kg ha}^{-1}$), as well as canopy cover and aboveground biomass evolution, in the
29 case of AquaCrop, whose goodness of fit indicators were close to 0.90 or higher. In terms
30 of crop evapotranspiration, AquaCrop simulated a 12% higher average value than
31 MOPECO. An in-depth analysis was performed to explain the differences.

32 **Keywords:** improved crop models parameterization, crop-water production function,
33 irrigation water productivity, ORDIL, water scarcity

35 1. Introduction

36 Worldwide, cereal crops occupy around 51% of the total growing area. In Spain, the
37 seventh largest cereal producer in Europe with a production of 5.8 million Mg in almost
38 2.6 million ha of cereal planted area (FAOSTAT, 2019), these commodities, especially
39 barley, are a key alternative for field agricultural systems. In semiarid regions, such as
40 the centre and south of Spain, where there is a clear tendency towards water resource
41 scarcity (Cramer et al., 2020), reductions in irrigation water abstraction in both Guadiana
42 and Júcar rivers basins in Castilla-La Mancha (CLM) region (Spain) are already a fact.
43 Applying deficit irrigation techniques (DI), either sustained (SDI) or regulated (RDI)
44 (Fereres and Soriano, 2007), during crop growth, would allow for irrigation strategies that
45 are able to improve crop irrigated water use, without causing significant yield losses. This
46 methodology would help mitigate climate change effects, maximize the production per
47 unit of water consumed, developing more resilient agricultural systems and limiting
48 desertification.

49 Several papers on the barley crop response to water deficit have reported that the end of
50 the vegetative period, flowering and yield formation are the most sensitive stages,
51 affecting the final crop yield and harvest quality (Abrha et al., 2012; Acevedo et al., 2002;
52 Cossani et al., 2009; Giunta et al., 1993; Ugarte et al., 2007). Barley crop water
53 requirements in CLM are around 400-500 mm, according to cycle length, which varies
54 between 155 and 210 days (Pardo et al., 2020), with the average irrigation water
55 requirements being 250 mm (JCRMO, 2020). Thus, the yield of irrigated barley is
56 between 4 and 5 times higher than under rainfed conditions (ITAP, 2020). However, the
57 current low profitability of this crop, and the increasing tendency of the water authority
58 to limit the volume of water for irrigation in the area (CHG, 2020; CHJ, 2020) are forcing
59 growers and technicians to adopt optimal irrigation techniques to reduce the use of
60 irrigation water with the aim of maximizing economic irrigation water productivity
61 (Pardo et al., 2020).

62 Several authors have developed algorithms for optimizing irrigation scheduling based on
63 the crop development and its productive response to water deficit (García et al., 2020;
64 Kloss et al., 2012; Kuschel-Otárola et al., 2018; Schütze et al., 2012), as well as on the
65 real-time readings obtained from weather stations and soil moisture sensors installed in
66 the field (Domínguez-Niño et al., 2020). One of these methodologies is called optimized
67 regulated deficit irrigation for limited volumes of irrigation water (ORDIL) (Domínguez
68 et al., 2012a; Leite et al., 2015), the main objective of which is to maximize yield at
69 harvest when the amount of available water is lower than the typical irrigation
70 requirements of the crop (Pardo et al., 2020). This methodology is based on the total
71 available volume of irrigation water at the beginning of the irrigation season, the
72 sensitivity of the crop to water deficit at its different development stages, the evolution of
73 climatic conditions, the amount of water received by the crop at each phenological stage
74 and the amount of irrigation water remaining for the following phenological stages until
75 physiological maturity.

76 Crop simulation models, when calibrated and validated, can be used as decision support
77 systems for the management of crops, farms or agricultural systems. Among other
78 functions, these models calculate the crop water requirements, determine the irrigation
79 scheduling and simulate crop yields according to the amount of irrigation water supplied
80 during crop development (de Wit et al., 2019; Pereira et al., 2003; Stöckle et al., 2014).
81 MOPECO (Ortega et al., 2004) and AquaCrop (Steduto et al., 2009) were designed to be
82 used by researchers and also by technicians and advanced farmers. Both models are based
83 on FAO methodology (Allen et al., 1998; Doorenbos and Kassam, 1979) and the number

84 of parameters required for the simulation of annual crops is low compared with other
85 models, as reported by López-Urrea et al. (2020), who calibrated the two models for a
86 barley crop using the data set of a three-year experiment carried out in Albacete province
87 (in the CLM region). MOPECO offers several options and tools that may be useful for
88 the management of actual irrigated farms, such as ORDIL, the effect of irrigation
89 uniformity on final yield (López-Mata et al., 2010) or the optimal distribution of crops
90 depending on the available amount of irrigation water and cultivable area (López-Mata et
91 al., 2016). AquaCrop is able to more precisely simulate the development of annual crops
92 and their final biomass depending on the climatic conditions and availability of water in
93 the soil during the growing cycle, providing irrigation scheduling strategies, such as full
94 irrigation, or allowing a certain soil water depletion level at which an irrigation event is
95 applied.

96 Therefore, the main aim of this research was to assess the applicability of both models as
97 decision support systems for barley crop under the semiarid climatic conditions of CLM.
98 To achieve this aim, the following partial objectives were proposed:

- 99 1. To improve the parametrization of both models for a barley crop developed by
100 López-Urrea et al. (2020), determining the average length of the different growing
101 stages of this crop for the different irrigated areas of CLM.
- 102 2. To compute and compare the crop-water production functions generated by the
103 tools and strategies provided by each model for the typical conditions of CLM.
- 104 3. To evaluate the accuracy of MOPECO and AquaCrop models by comparing their
105 results with those obtained in a three-year experiment conducted in Albacete,
106 where the ORDIL methodology was applied to a barley crop (Pardo et al., 2020).

107 **2. Material and methods**

108 **2.1. Description of crop models. Approach simulation**

110 The AquaCrop model (Steduto et al., 2009) maintains the original concept proposed in
111 FAO-33 (Doorenbos and Kassam, 1979) but, in this case, it estimates biomass production
112 from actual crop transpiration through the normalized water productivity (WP) parameter
113 (Steduto et al., 2012), since the model separates soil evaporation from crop transpiration
114 as is also done by FAO-56 methodology (Allen et al., 1998; Pereira et al., 2021a). Crop
115 cycle length is determined by days after sowing (DAS), or calculated by using the
116 growing degree days methodology (GDD, °C). Finally, crop yield is estimated from the
117 biomass production and the harvest index. Several stress coefficients (soil water, air
118 temperature, soil fertility and soil salinity) are used to adjust the daily green canopy cover,
119 crop transpiration, above-ground biomass and yield formation. AquaCrop model is now
120 designed to be used with annual crops, whose conservative crop parameters are provided
121 in the AquaCrop software for many species (maize, barley, wheat, cotton, rice, soybean,
122 potato, sunflower, tomato, among others; Vanuytrecht et al. 2014). AquaCrop can be used
123 to report the role of different soil-climate systems in water-limited crop production as
124 well as the analysis of different scenarios, such as climate change, water supply, crop
125 type, field management, etc. (Vanuytrecht et al., 2014). In addition, the AquaCrop plug-
126 in program (Raes et al., 2017) and AquaCrop-GIS (Lorite et al., 2013), together with
127 AquaCrop-OS, the open source version (Foster et al., 2017), allow the simulation time to
128 be significantly reduced when both a larger number of simulations are carried out and
129 interpretation and analysis of the results is complex (Vanuytrecht et al., 2014).

130 MOPECO was conceived to optimize the gross margin of farms through the use of deficit
131 irrigation strategies (De Juan et al., 1996). It is based on FAO-33 (Doorenbos and
132 Kassam, 1979) and FAO-56 (Allen et al., 1998; Pereira et al., 2020, 2021b)

133 methodologies. For the simulation of yield, the model determines the ratio between actual
134 and potential (maximum) crop evapotranspiration (ET_a and ET_m , respectively) for each
135 growing stage (Domínguez et al., 2011), where soil evaporation and crop transpiration
136 components are not separated. Similarly to AquaCrop, the crop development is simulated
137 using both DAS and GDD. Yields for different amounts of irrigated water supplied to the
138 crop are used to determine the “yield vs. irrigation depth” function. The simulation of the
139 irrigation water allocation during the growing period is determined by the optimized
140 regulated deficit irrigation (ORDI) methodology. ORDI maximizes yield for a certain
141 water deficit target by determining the ET_a/ET_m ratios to be applied at each growing stage
142 (Domínguez et al., 2012a). Under real management conditions, where climatic conditions
143 for the growing period are unknown and the amount of available irrigation water is
144 limited, MOPECO uses the ORDIL methodology (Leite et al., 2015). Both methodologies
145 have been applied to different crops: maize (Domínguez et al., 2012a), onion (Domínguez
146 et al., 2012b), garlic (Domínguez et al., 2013; Sánchez-Virosta et al., 2020), carrot
147 (Carvalho et al., 2014), melon (Leite et al., 2015), potato (Martínez-Romero et al., 2019)
148 and barley (Pardo et al., 2020).

149 **2.1.1. AquaCrop model. Irrigation water scheduling**

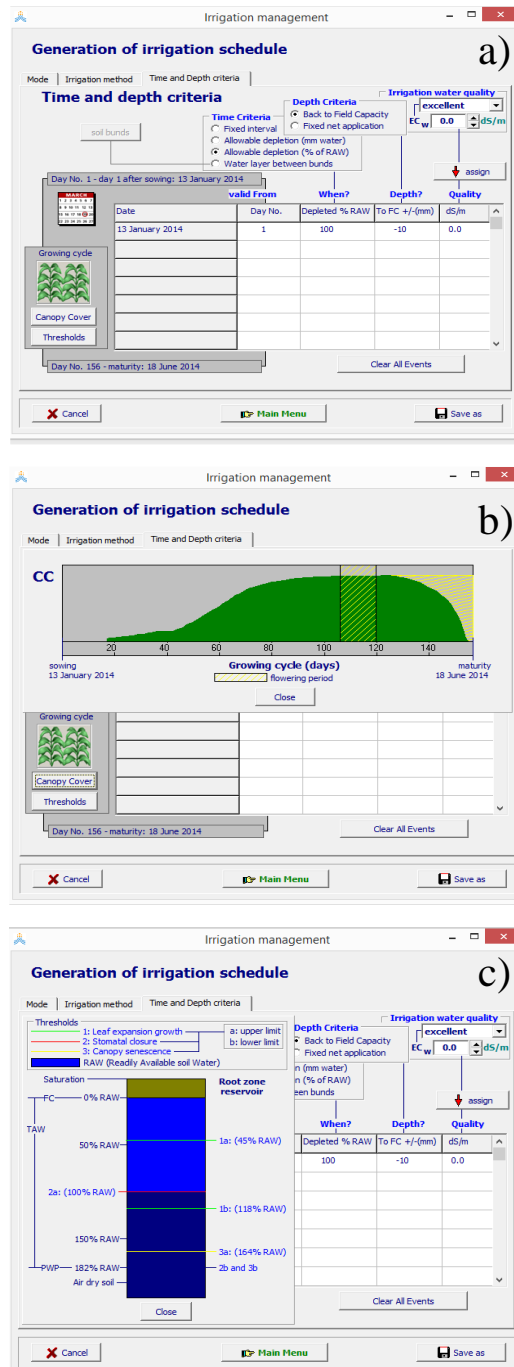
150 When the actual crop evapotranspiration (ET_a) is calculated, the AquaCrop model
151 separates the soil water evaporative component from the crop transpiration (Steduto et
152 al., 2009). Thus, this model takes into account both the water inputs (net irrigation, rainfall
153 and capillary rise) and outputs (runoff, deep percolation and ET_a) at the crop root zone in
154 order to compute a daily soil water balance. An accurate description of the soil water
155 movement is made by dividing soil depth into several compartments, with the thickness
156 of each one being variable according to user specifications. The AquaCrop manual (Raes
157 et al., 2018) shows a detailed description and the algorithms used to calculate the soil
158 water balance.

159 From that balance, AquaCrop model simulates the irrigation management in three
160 alternative ways: a) by resolving the net irrigation water requirements of the crop, keeping
161 the soil water depletion at the root zone above a threshold, which is delimited by the user
162 (generally 50% of the readily available water, RAW). These requirements do not take
163 into account the irrigation uniformity effect; b) by considering a previously designed
164 irrigation schedule where each irrigation event is specified by the user; thus, date of
165 irrigation event, net irrigation depth and the quality of water (electric conductivity, ECw)
166 must be given for each irrigation event; c) by allowing AquaCrop to automatically
167 generate an irrigation schedule according to the criteria established by the user.

168 In the third alternative, users define in AquaCrop the way an irrigation event must be
169 simulated. Thus, two criteria are considered: (i) when the irrigation event has to be
170 triggered (irrigation time criterion, ITC), and (ii) how much water has to be applied
171 through the irrigation system (irrigation depth criterion, IDC), being specified to either
172 all the crop cycle or a certain period of time (Fig. 1a). The ITC can be established by the
173 user, who either fixes a constant number of interval days between irrigation events or
174 selects a soil water depletion threshold (either mm of water or % of RAW; Fig. 1a). The
175 IDC also offers two options, namely, to refill the soil water content up to field capacity
176 or to fix a constant net irrigation depth (mm) (Fig. 1a). The former option allows over-
177 irrigation (uniformity of irrigation system) or under-irrigation (erratic rainfall
178 distribution) to be considered.

179 Finally, in this third method, which also considers water quality, users cannot generate an
180 irrigation schedule, coordinating two different options for each criterion along the crop

181 cycle, either the ITC or IDC. Graphically, users may compose their own irrigation
 182 strategy according to the crop growth stage (initial, development, mid-season, flowering
 183 and late season; Fig. 1b) and the different soil water stress thresholds (mainly leaf
 184 expansion growth, stomatal closure and canopy senescence, Fig. 1c).



185 Figure 1. Generation of irrigation schedule with AquaCrop (a) establishing criteria from
 186 the different phenological stages along the growing cycle (b) or by available soil water
 187 thresholds (c).

188 Finally, the model distinguishes between different wetted soil fractions, depending on the
 189 irrigation system considered. Thus, the percentage of the wetted soil surface fluctuates
 190 from 100% (sprinkler, border and basin irrigation) to 0% (subsurface drip irrigation), with

191 intermediate values for other irrigation systems (30-100% in furrow irrigation and 15-
192 40% in trickle (drip)-micro irrigation).

193

194 **2.1.2. MOPECO model. Irrigation water scheduling**

195 MOPECO calculates the daily soil water content in the root area following the FAO-56
196 approach (Allen et al., 1998), balancing inputs (net irrigation, precipitation, and deep
197 water reached by roots) and outputs (runoff, crop evapotranspiration and deep
198 percolation) (Domínguez et al., 2011). In this sense, MOPECO computes the total
199 available water (TAW) in the root zone, understanding TAW as the difference in soil
200 water content between field capacity and permanent wilting point; and considers a
201 depletion fraction “p” threshold which is the fraction of TAW that a crop can extract
202 without suffering water stress (Allen et al., 1998; Domínguez et al., 2011).

203 In addition, the MOPECO irrigation scheduling module requires as input data: (i) the
204 interval of maximum and minimum irrigation depth that can be supplied by the irrigation
205 system per irrigation event (MID and mid, respectively); (ii) minimum and maximum
206 number of interval days to trigger an irrigation event; (iii) maximum level of soil water
207 content that can be refilled by an irrigation event (% TAW) with the aim of decreasing or
208 avoiding percolation when there is unexpected rainfall after an irrigation event.

209 Thus, three situations can be distinguished: a) maintaining no water deficit along the crop
210 cycle, when the soil water content is always higher than p and the irrigation water depth
211 per event is calculated, in order to refill the soil water content in an intermediate point
212 between field capacity and $(1-p)*TAW$ (%TAW selected by the user); b) reaching a
213 certain global water deficit level for the complete crop cycle (global ET_a/ET_m ratio
214 defined by the user), with MOPECO aiming to determine the water deficit level to be
215 caused to the crop at each phenological stage in order to maximize final yield; and c)
216 distributing a certain volume of irrigation water during the crop cycle according to the
217 water deficit level for each phenological stage that maximizes yield without exceeding
218 the limited volume according to the progress of climatic conditions. In situations b) and
219 c), MOPECO calculates the daily accumulated ET_a/ET_m ratio from the beginning up to
220 the end of each growth stage. If the daily accumulated ET_a/ET_m ratio at a certain date is
221 higher than the ET_a/ET_m target ratio for that stage, MOPECO does not apply any irrigation
222 unless the maximum number of days without water supply (irrigation or rainfall) is
223 reached, or the daily ET_a/ET_m ratio reaches a minimum value fixed by the user (0.35 is
224 recommended), to avoid excessive depletion of soil moisture. (Domínguez et al. 2011).
225 The global ET_a/ET_m ratio of each crop growth stage is established following the ORDI
226 and ORDIL methodologies (Domínguez et al., 2012a; Leite et al., 2015; Pardo et al.,
227 2020), which produces the highest crop yield for a certain overall deficit target or for a
228 limited irrigation water volume, using non-linear optimization software such as Solver
229 (Microsoft, 2018). MOPECO is sometimes unable to attain the target deficit rate proposed
230 for each growth stage by the user or by the optimizer. In these cases, the irregular
231 distribution of rainfall and/or the high soil water content at the beginning of the simulation
232 are the main causes of this mismatch between the objective and the final deficit rate.

233 **2.1.3. Model parameterization**

234 López-Urrea et al. (2020) described in detail the parameterization of both models (Table
235 1) for barley crop growth under different irrigation regimes, using the data of a three year
236 experiment (from 2011 to 2013) conducted under the semiarid conditions of Albacete
237 province (Fig. 2).

238 Table 1. Specific parameters of barley crop for AquaCrop and MOPECO models.

Model	Parameter	Value
AquaCrop	Crop growth and development	
	Base temperature, °C	2
	Upper temperature threshold, °C	28
	Canopy size of the seeding, cm ² plant ⁻¹	1.50
	Canopy growth coefficient, % °C ⁻¹ day ⁻¹	0.014
	Canopy decline coefficient, % °C ⁻¹ day ⁻¹	0.644
	Water productivity, g m ⁻²	18.5
	Crop transpiration coefficient	1.10
	Yield formation	
	Reference Harvest Index, % ^{NC}	54
	Soil water stress	
	Possible increase in HI caused by water stress before flowering, %	6
	Positive impact of restricted vegetative growth during yield formation on HI	10 (small)
	Negative impact of stomatal closure during yield formation on HI	7 (moderate)
	Upper threshold for canopy expansion	0.25
	Lower threshold for canopy expansion	0.65
	Upper threshold for stomatal closure	0.55
	Upper threshold for early canopy senescence	0.85
	Shape factor for canopy expansion	3.0
	Shape factor for stomatal closure	3.0
	Shape factor for early canopy senescence	3.0
Upper threshold for pollination failure	0.90	
MOPECO	Kc	
	- Stage I	0.30
	- Stage II	0.30-1.15
	- Stage III	1.15
	- Stage IV	1.15-0.45
	Ky	
	- Stage i	0.20
	- Stage ii	0.55
	- Stage iii	0.30
	- Stage iv	0.15
Ym (x10 ³ kg/ha)	9.000	
Base temperature, °C	2	
Upper temperature threshold, °C	28	

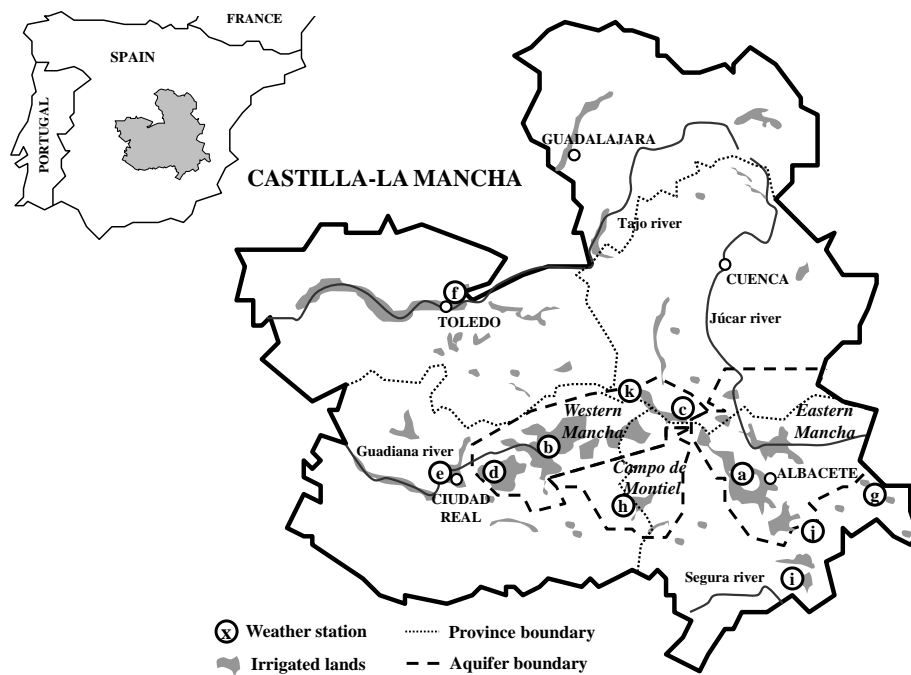
where Stage I: Initial; Stage II: Crop development; Stage III: Mid-season; Stage IV: Late season; Stage i: Vegetative period, which included establishment (Ky i') and vegetative development (Ky i'') periods; Stage ii: Flowering period; Stage iii: Yield formation; Stage iv: Ripening.

239

240 2.2. Description of the study area

241 The study area is located in southeast Spain in a semiarid area where around 70% of water
 242 resources used for irrigated crops are from groundwater (Domínguez and De Juan, 2008).
 243 The three main affected aquifers are Eastern Mancha, Western Mancha and Campo de
 244 Montiel, whose irrigated area is around 350,000 ha distributed over 29,000 km² (Fig. 2).
 245 Irrigated barley crop is usually managed under a sprinkler irrigation system because the
 246 seasonal average rainfall is between 300-350 mm year⁻¹, from September to June, and
 247 with high reference evapotranspiration (~1150 mm year⁻¹) (Domínguez et al., 2013).

248 The typical soils in this area are characterized by shallow depths (0.40-0.55 m) which are
 249 limited by a somewhat fragmented limestone sedimentary rock. They have a slightly basic
 250 pH (7.5-8.5), low organic matter content (1.2-1.6%) and their general texture is classified
 251 as loam or sandy clay loam soils (Domínguez and De Juan, 2008).



252

253 Figure 2. Location of the main irrigated areas in Castilla-La Mancha region.

254

255 2.3. Crop cycle length influenced by climatic variability

256 To determine the average length of the barley crop cycle, as well as its development stages
 257 in the study area, 28 crop phenological monitoring studies, carried out by the Irrigation
 258 Advisory Service (IAS) of CLM (SIAR-CLM, 2014), were used. This monitoring work
 259 included the four main irrigable areas (Fig. 2) over 11 cropping seasons, where short cycle
 260 varieties of barley were mainly studied since they are mostly grown under irrigated
 261 conditions (sowing date by mid-January and harvest date at the end of June). The BBCH-
 262 scale (Bleiholder et al., 2001) was used to determine the phenological growth stages of
 263 barley related to the input parameters required by both models (canopy development, mid-
 264 season and late season for AquaCrop; Kc and Ky coefficients for MOPECO; Table A1,
 265 Annex).

266 The thermal time duration of the barley growth stages in terms of accumulated GDD was
 267 obtained for both models. AquaCrop establishes three different methods to calculate GDD
 268 (Mcmaster and Wilhelm, 1997), with the first method (Raes et al., 2018) being used for
 269 simulations, while MOPECO uses the double triangulation method (Sevacherian et al.,
 270 1977) which is suitable in the area. The mean accumulated GDD value for each growth
 271 stage of barley was calculated taking into account the base temperature (T_B) and the upper
 272 temperature (T_U) thresholds. Combining a set of values reported from several studies
 273 (from 0 °C to 10 °C and from 20 °C to 38 °C, for T_B and T_U , respectively; López-Bellido
 274 1991; Juskiw et al. 2001; Araya et al. 2010; Abrha et al. 2012) and those shown in Table
 275 1, the selected final threshold values were derived from the lowest standard deviation and
 276 coefficient of variation GDD data for all monitoring barley growth stages.

277 2.4. Typical meteorological year

278 A typical meteorological year (TMY) represents the conditions considered “typical” over
 279 a long period of time, and consists of 12 months selected from individual years and
 280 concatenated to form a complete year with daily values (Pardo et al., 2020). In this study,
 281 an intermediate TMY (TMY_{intermediate}), determined by Leite et al. (2015) with a weather

282 station located in the experimental area (Albacete, southeast Spain ; Fig. 2), was used.
283 The main values computed for $TMY_{intermediate}$ were $1212 \text{ mm year}^{-1}$ and 289 mm year^{-1}
284 for reference evapotranspiration (ET_0) computed using the FAO56 Penman-Monteith
285 equation (Allen et al., 1998) and precipitation, respectively.

286 **2.5. Simulating the crop barley yield response to irrigation management**

287 Using the GDD methodology already described and applied for a $TMY_{intermediate}$ in the
288 study area (Leite et al., 2015), the crop barley yield and irrigation water productivity
289 (IWP; expressed as kg of commercial crop yield per m^{-3} of irrigation water supplied to
290 the crop) response to irrigation scheduling were simulated with AquaCrop and MOPECO.
291 The derived crop-water and IWP-water production functions were compared to evaluate
292 the performance of both irrigation scheduling tools.

293 Four irrigation strategies (IS) were designed to be implemented in the AquaCrop model
294 (IS1_Aq, IS2_Aq, IS3_Aq and IS4_Aq). The four strategies were considered as sustained
295 irrigation through the simulated crop cycle. In two of the IS strategies (IS1_Aq and
296 IS2_Aq), a time criterion was fixed with an interval time between 1 to 27 days, where
297 odd days were used, obtaining 14 simulations for each IS (Table 2). The depth criteria of
298 these IS was different: IS1_Aq applied, at each irrigation event, 23.5 mm of gross water
299 depth; while IS2_Aq refilled the soil water content up to field capacity minus 10 mm as
300 a margin for unexpected rainfall events. The other two IS strategies (IS3_Aq and IS4_Aq)
301 considered the irrigation event was triggered when a certain soil water content was
302 depleted (represented as mm), being 12 simulations per each IS (Table 2), and following
303 the same irrigation depth criteria previously described, i.e. to apply 23.5 mm per irrigation
304 event (IS3_Aq), and to refill up to field capacity minus 10 mm (IS4_Aq).

305 The gross irrigation depth of 23.5 mm was established since it is the most widely used
306 according to the representative farm area and the daily irrigation time normally used. In
307 addition, barley crop yield was also simulated under rainfed conditions in order to find
308 the ordinate of the crop-water production function. Finally, the regulated deficit irrigation
309 scheduling, taking into account crop growth stages, was not analysed because of the huge
310 number of combinations which may be derived, surpassing, in this case, the goals for
311 managing this model by an intermediate user.

312 In the case of MOPECO, two irrigation strategies were performed (IS1_ORDI and
313 IS2_ORDIL; Table 2). The first strategy established an optimized regulated deficit
314 irrigation with ten global ET_a/ET_m ratio objectives (between 1.00 y 0.55) (Table 2). To
315 simulate the ORDIL irrigation strategies (IS2_ORDIL), ten gross irrigation water
316 amounts were fixed as the input data model, which derived in different global ET_a/ET_m
317 ratios (Table 2). In the former IS, the maximum simulated irrigation water amount had a
318 global ET_a/ET_m ratio equal to 1.00 (i.e. the same total irrigation depth simulated in
319 IS1_ORDI, 312 mm), and the rest of simulations were run for irrigation depths
320 differentiated at intervals of 20 mm (Table 2). A total of 15 and 2 days were established
321 as maximum and minimum intervals between irrigation events when no rainfall occurs.
322 The gross irrigation water depth per event was set between 4 and 30 mm.

323 For the simulations, the sowing date was January 13th, the maximum root depth was 1.0
324 m although its development was limited by the root restrictive layer (0.40 m). The
325 physical and hydraulic soil characteristics were those measured by Pardo et al. (2020)
326 which are representative of this production area. Both models were run in GDD mode,
327 using the average GDD for each growth stage from the GDD methodology previously
328 described, and using the parameterized coefficients shown in Table 1. In this work, a
329 value equal to 85% of irrigation efficiency was established, corresponding to a sprinkler

330 irrigation system. The initial soil water content was established at 80% of field capacity.
331 In the case of AquaCrop, the simulated dry matter yield outputs were normalized to
332 standard commercial yields (12% of moisture content), since yield outputs computed by
333 MOPECO are given as commercial yield.

334

Table 2. Irrigation strategies simulated by AquaCrop (Aq) and MOPECO (ORDI and ORDIL strategies) and both computed crop yield and crop-water flux results.

IS	AqC	MoC	MIWD	IE	GIWD	RO	DP	Y	IWP	ET _a	ET _a /ET _m
IS1_Aq	1	-	23.5	157	3694	51	2797	6.806	0.184	321	0.714
	3	-	23.5	52	1224	51	612	11.676	0.954	448	0.998
	5	-	23.5	31	729	42	218	11.658	1.598	447	0.994
	7	-	23.5	22	518	41	88	11.275	2.178	425	0.944
	9	-	23.5	17	400	23	34	10.647	2.662	405	0.900
	11	-	23.5	14	329	25	9	9.688	2.941	368	0.818
	13	-	23.5	12	282	23	0	9.230	3.269	342	0.760
	15	-	23.5	10	235	20	0	8.245	3.504	330	0.733
	17	-	23.5	9	212	18	0	7.506	3.544	318	0.706
	19	-	23.5	8	188	30	0	6.541	3.475	288	0.642
	21	-	23.5	7	165	14	0	6.478	3.933	295	0.656
	23	-	23.5	6	141	18	0	6.733	4.769	279	0.624
	25	-	23.5	6	141	15	0	5.590	3.959	280	0.624
27	-	23.5	5	118	16	0	5.761	4.897	266	0.591	
IS2_Aq	1	-	3.4	99	393	37	0	11.685	2.971	445	0.990
	3	-	9.4	38	387	39	0	11.685	3.016	443	0.984
	5	-	12.9	26	378	38	0	11.670	3.086	440	0.978
	7	-	18.3	17	368	42	0	11.384	3.094	429	0.953
	9	-	19.5	14	328	25	0	11.114	3.385	414	0.920
	11	-	19.3	13	303	32	0	10.549	3.485	384	0.854
	13	-	18.9	12	274	20	0	10.205	3.721	366	0.813
	15	-	22.6	9	255	18	0	9.265	3.632	363	0.807
	17	-	23.1	8	235	15	0	8.458	3.595	345	0.768
	19	-	22.0	8	224	29	0	7.831	3.496	323	0.719
	21	-	22.5	7	203	14	0	8.041	3.958	328	0.729
	23	-	16.5	6	129	18	0	6.327	4.921	268	0.597
	25	-	23.7	6	188	12	0	7.185	3.822	313	0.694
27	-	23.7	5	161	20	0	7.481	4.648	301	0.667	
IS3_Aq	12.3	-	23.5	21	494	45	35	11.685	2.365	435	0.967
	27.3	-	23.5	15	353	16	0	11.681	3.310	431	0.958
	29.5	-	23.5	15	353	20	0	11.680	3.309	430	0.957
	31.7	-	23.5	14	329	25	0	11.600	3.521	420	0.935
	34.0	-	23.5	14	329	18	0	11.413	3.465	416	0.925
	36.2	-	23.5	13	306	33	0	10.459	3.419	398	0.887
	38.4	-	23.5	12	282	19	0	9.742	3.450	387	0.863
	40.7	-	23.5	11	259	18	0	8.463	3.270	364	0.811
	42.9	-	23.5	9	212	16	0	8.038	3.795	341	0.760
	45.1	-	23.5	8	188	14	0	6.631	3.523	313	0.698
	47.4	-	23.5	5	118	13	0	4.753	4.040	266	0.589
49.6	-	23.5	4	94	13	0	4.434	4.711	247	0.546	
IS4_Aq	12.3	-	4.8	86	393	37	0	11.685	2.972	445	0.989
	27.3	-	18.0	17	361	29	0	11.619	3.218	436	0.970
	29.5	-	20.0	14	337	19	0	11.597	3.438	431	0.958
	31.7	-	23.5	11	319	16	0	11.630	3.641	421	0.936
	34.0	-	25.2	10	314	14	0	11.550	3.680	417	0.927
	36.2	-	27.5	9	313	28	0	10.782	3.444	403	0.897
	38.4	-	29.4	8	302	31	0	9.839	3.253	388	0.863
	40.7	-	30.9	6	248	24	0	8.940	3.610	358	0.798
	42.9	-	31.2	5	215	12	0	7.766	3.619	337	0.750
	45.1	-	31.5	4	180	19	0	7.272	4.029	313	0.697
	47.4	-	30.2	3	139	14	0	5.177	3.736	270	0.599
49.6	-	30.3	3	139	19	0	4.885	3.513	254	0.563	
IS1_OR DI	-	1.00	19.5	16	312	37	5	11.664	3.740	384	0.999
	-	0.95	17.2	18	310	37	20	11.220	3.619	367	0.961
	-	0.90	14.8	18	266	37	8	11.084	4.167	360	0.934
	-	0.85	9.8	25	244	37	4	10.520	4.311	346	0.903

-	0.80	10.2	23	234	37	4	10.174	4.343	338	0.876	
-	0.75	9.9	22	217	37	4	9.606	4.430	322	0.830	
-	0.70	10.2	19	194	37	4	9.101	4.697	305	0.784	
-	0.65	9.9	18	179	37	4	8.604	4.808	292	0.743	
-	0.60	8.4	18	151	37	4	7.727	5.103	270	0.696	
-	0.55	6.0	22	131	37	4	7.123	5.435	252	0.657	
<hr/>											
IS2_ORDIL	-	312	19.5	16	312	37	5	11.664	3.740	384	0.999
	-	292	12.1	24	292	37	4	11.281	4.039	370	0.955
	-	271	13.5	20	271	37	8	10.934	4.039	359	0.936
	-	246	9.4	26	246	37	4	10.528	4.286	347	0.899
	-	232	8.3	28	232	37	4	10.205	4.408	337	0.878
	-	210	8.1	26	210	37	4	9.612	4.569	319	0.836
	-	190	10.0	19	190	37	4	8.936	4.701	302	0.794
	-	170	7.7	22	170	37	4	8.368	4.909	286	0.760
	-	149	8.3	18	149	37	4	7.687	5.156	268	0.701
	-	131	6.9	19	131	37	4	7.116	5.437	253	0.656
<hr/>											
RAINFED	-	-	-	-	-	12	0	2.800	-	177	0.398

337 IS: irrigation strategy; AqC: irrigation event criterion by AquaCrop (IS1_Aq and IS2_Aq: number of interval days;
338 IS3_Aq and IS4_Aq: depleted mm threshold); MoC: irrigation event criterion by MOPECO (IS1_ORDI: global ET_a/ET_m
339 ratio (dimensionless); IS2_ORDIL: limited volumes of irrigation water (mm)); IE: number of irrigation events; MIWD:
340 mean gross irrigation water depth per event (mm); GIWD: total gross irrigation water depth (mm), considering 85%
341 irrigation efficiency; RO: runoff (mm); DP: deep percolation (mm); Y: crop yield (12% of water content; $\times 10^3$ kg ha⁻¹);
342 IWP: irrigation water productivity (kg m⁻³); ET_a : actual crop evapotranspiration (mm); ET_m : maximum crop
343 evapotranspiration.

344

345 2.6. Experimental dataset using the ORDIL methodology

346 Evaluating the performance of the AquaCrop and MOPECO models, as well as their inter-
347 comparison, we used several irrigation schedules generated by ORDIL methodology with
348 a limited total irrigation depth (Pardo et al., 2020). Pardo et al. (2020) conducted the field
349 trials in 2015, 2016 and 2017 on an experimental farm located in Albacete (SE Spain). Its
350 geographic coordinates are 1° 53' 58" W, 38° 56' 42" N, and the altitude is 695 m above
351 mean sea level. Five treatments of ORDIL irrigation strategies were carried out to analyse
352 their effects on both IWP and crop yield in the "Shakira" barley cultivar. A control
353 treatment (no water deficit, ND) received the full crop water requirements following
354 López-Urrea et al. (2020), while the other four irrigation treatments received a percentage
355 of the net typical irrigation water requirements (T100, 100%; T90, 90%; T80, 80% and
356 T70, 70%) which were adjusted to 2500 m³ ha⁻¹ (Pardo et al. 2020). All irrigation
357 schedules were obtained from Pardo et al. (2020). Those authors carried out four
358 optimizations during the crop cycle length (one per each K_y stage; Table 1) in order to
359 maximize crop yield according to the water deficit (in terms of ET_a/ET_m) applied to each
360 barley K_y stage.

361 The soil of the experimental plot, classified as clay-loam, was a shallow soil (0.40 m of
362 average soil depth), whose available water content was 0.124 cm³ cm⁻³ (0.313 cm³ cm⁻³
363 for field capacity and 0.189 cm³ cm⁻³ for permanent wilting point). During the three
364 experimental cropping seasons, ET_o was between 12.5% and 25.0% higher than the
365 TMY_{intermediate} (400 mm), while the total precipitation was lower for 2015 and 2016
366 experimental seasons (around 20%) and slightly higher for 2017 season (5%) with respect
367 to the TMY_{intermediate} (165 mm) (Pardo et al., 2020). Real-time ET_a/ET_m optimizations for
368 each K_y crop stage were fitted to the weather conditions occurring during the current year.
369 The total water received by crop (rainfall and irrigation) and crop yield obtained for each
370 treatment and experimental seasons are shown in Table 3 (Pardo et al., 2020).

371 In addition, for each irrigation treatment, during the three experimental seasons, both the
372 total crop biomass and the leaf area index (LAI) evolutions were measured
373 (approximately every 15 days in two subplots of each treatment). Two samples of
374 0.5×0.5m were collected and measured per treatment by using an electronic meter device
375 (LI-COR-3100C, Licor, Inc., Lincoln, NE) to determine LAI and were introduced into
376 an oven at 70 °C up to constant weight for crop biomass. Crop canopy cover (CC) was
377 estimated from the measured LAI using the Ritchie equation (Ritchie et al., 1985), where
378 the extinction coefficient was established as 0.60.

$$379 \quad CC = 1 - \exp(-K \cdot LAI) \quad (1)$$

380 where CC is canopy cover; K is extinction coefficient; LAI is leaf area index.

381

382 Table 3. Total water received by the crop, commercial yield (12% grain moisture content) obtained at harvest and aboveground biomass and canopy
 383 cover evolution during the three experimental seasons.

Treatment	Experimental year 2015					Experimental year 2016					Experimental year 2017						
	ND	100%	90%	80%	70%	ND	100%	90%	80%	70%	ND	100%	90%	80%	70%		
Tw (mm)	419.1	384.1	358.6	333.7	308.8	463.8	388.8	355.4	330.8	305.9	541.7	423.8	398.9	375.5	348.6		
GIWD (mm)	285.6	250.6	225.1	200.2	175.3	333.4	258.4	225	200.4	175.5	367.9	250	225.1	201.7	174.8		
Obs. Yield* (SD)	9.199 (0.619) [#]	8.616 (0.457)	7.620 (0.362)	7.367 (0.169)	6.404 (0.492)	8.877 (0.296)	7.985 (0.301)	7.690 (0.444)	7.214 (0.215)	6.331 (0.148)	9.071 (0.511)	8.032 (0.398)	7.621 (0.250)	7.311 (0.232)	6.283 (0.295)		
DAS	Aboveground biomass (x10³ kg ha⁻¹)					DAS	Aboveground biomass (x10³ kg ha⁻¹)					DAS	Aboveground biomass (x10³ kg ha⁻¹)				
0	0.000	0.000	0.000	0.000	0.000	0	0.000	0.000	0.000	0.000	0.000	0	0.000	0.000	0.000	0.000	0.000
63	0.492	0.492	0.492	0.492	0.492	64	0.9382	0.914	0.9504	0.904	0.8683	77	2.713	2.713	2.4116	2.4116	2.4116
73	1.328	1.328	1.328	1.328	1.328	85	3.6294	3.6468	3.5746	3.5488	3.523	98	7.3166	7.3166	6.8856	6.8856	6.8856
88	4.016	4.016	4.016	4.016	4.016	98	7.5706	7.1241	5.8648	5.775	5.6852	111	10.418	10.239	10.242	9.7012	9.2638
102	7.066	7.066	6.927	6.282	6.066	110	9.7844	9.5912	8.4066	8.0114	7.3342	129	14.509	14.878	13.224	14.02	12.858
114	11.978	11.978	10.52	10.02	9.312	126	11.553	11.553	10.887	10.006	9.3018	146	19.329	16.868	17.272	17.766	16.712
127	16.382	16.382	15.379	14.674	13.963	140	16.7	14.571	13.889	13.737	12.673	150	18.135	15.831	14.923	14.017	11.171
153	16.291	13.859	13.114	12.503	11.187	158	13.92	11.175	10.412	10.136	8.087	-	-	-	-	-	-
DAS	Canopy cover (%)					DAS	Canopy cover (%)					DAS	Canopy cover (%)				
0	0.0	0.0	0.0	0.0	0.0	0	0.0	0.0	0.0	0.0	0.0	0	0.0	0.0	0.0	0.0	0.0
56	11.0	11.0	11.0	11.0	11.0	42	11.0	11.0	11.0	11.0	11.0	50	11.0	11.0	11.0	11.0	11.0
63	35.4	35.4	35.4	35.4	35.4	64	49.1	48.7	49.4	48.4	47.1	98	95.0	95.0	93.1	93.1	93.1
73	57.1	57.1	57.1	57.1	57.1	85	94.2	94.3	93.8	93.6	93.4	111	98.4	98.4	97.6	97.6	97.6
88	97.6	97.6	97.6	97.6	97.6	98	99.7	99.5	96.7	95.9	95.6	129	99.3	99.2	98.6	98.7	97.8
102	99.8	99.8	99.6	99.5	99.1	110	97.9	96.8	95.4	93.0	89.8	146	92.8	93.4	91.1	92.7	87.1
114	99.9	99.9	99.8	99.6	99.3	126	92.0	91.3	88.6	82.9	74.0	-	-	-	-	-	-
127	99.5	99.5	99.2	99.0	98.8	140	79.9	71.5	65.2	36.7	35.2	-	-	-	-	-	-
153	82.4	82.4	83.2	40.8	37.1	158	0.0	0.0	0.0	0.0	0.0	-	-	-	-	-	-

384 Tw: total water received (irrigation + total rainfall); GIWD: gross irrigation water depth; Obs. Yield: observed yield (x10³ kg ha⁻¹); *: yield performed against yield commercial grain (12% of
 385 water content); #: values between brackets are the standard deviation (SD); DAS: days after sowing.

386

387

388

389 **2.7. Statistical analysis to evaluate the irrigation schedule tools and model**
 390 **performance**

391 Several statistical indicators were performed to estimate the goodness of fit for both
 392 simulated crop-water and the IWP-water production function of each IS (CWPF and
 393 IWPPF, respectively), with the gross irrigation-water depth (GIWD) being the dependent
 394 variable in both functions. Curvilinear and lineal models were used to fit these functions
 395 (Saseendran et al., 2015; Stewart and Hagan, 1973), since a portion of the applied water
 396 is not used in evapotranspiration and is lost in different process (Feres and Soriano,
 397 2007). Thus, the coefficient of determination (R^2), the significance of both model
 398 parameters and R^2 (p-value), as well as the standard error (SE) of estimate of the
 399 regression model were analysed. Statgraphics® Centurion XVII software was used to
 400 calculate these statistics.

$$401 \quad Z = a + b \cdot GIWD + c \cdot GIWD^2 \quad (2)$$

$$402 \quad Z = a + b \cdot GIWD \quad (3)$$

403 where Z is the commercial crop yield (Y; kg ha⁻¹) or irrigation water productivity (IWP;
 404 kg m⁻³); a, b, c are the model's coefficients; GIWD is the gross irrigation water depth
 405 (mm).

406 With respect to the performance of both models in simulating three experimental trials
 407 under ORDI methodology, the statistical parameters used to determine the goodness of
 408 fit of the simulations were: root mean square error (RMSE), mean bias error (MBE),
 409 efficiency model (EF), and index of agreement (d; Willmott 1982).

$$410 \quad RMSE = [n^{-1} \cdot \sum(S_i - O_i)^2]^{1/2} \quad (4)$$

411 where RMSE is the Root Mean Square Error; n, is the number of observations; S_i and O_i
 412 are the simulated and observed values, respectively.

$$413 \quad MBE = n^{-1} \sum_{i=1}^n (S_i - O_i) \quad (5)$$

414 where MBE is the mean bias error.

$$415 \quad EF = 1 - \frac{\sum(S_i - O_i)^2}{\sum(O_i - \bar{O})^2} \quad (6)$$

416 where EF is the efficiency model.

$$417 \quad d = 1 - \left(\frac{\sum(S_i - O_i)^2}{\sum((S_i - \bar{O}) + (O_i - \bar{O}))^2} \right) \quad (7)$$

418 where d is the index of agreement.

419 RMSE was used to analyse the variance of the error, which ranges from 0 to positive
 420 infinity, with the former indicating good, and the latter poor, model performance. The
 421 MBE expresses the average size of the estimated errors and was used to indicate the
 422 under- or overestimations of the model. Finally, the EF and d statistics (non-dimensional)
 423 were used as the indicator of model quality, where values close to 1 mean there is a good
 424 agreement. EF ranges between -∞ to 1, while d index ranges between 0 and 1. These
 425 statistics were computed using the number of independent observations for each treatment
 426 for canopy cover and biomass progression (only with AquaCrop). However, those
 427 statistics were calculated for standard commercial yield (12% of water content) with the
 428 data set obtained from the five treatments during the three experimental seasons (both
 429 AquaCrop as MOPECO). Finally, the differences between observed and simulated yield
 430 values were computed to estimate the performance model following the criteria

431 established by a number of authors (differences between simulated and observed data
 432 lower than 10% and with more than 70% of cases achieving the former percentage;
 433 (Domínguez et al., 2012c; Farahani et al., 2009; Heng et al., 2009; López-Urrea et al.,
 434 2020).

435 3. Results and discussion

436 3.1. Duration of barley growing stages in Castilla-La Mancha

437 Analysing the barley growth stages with all monitoring field data, the lowest values of
 438 standard deviation and coefficient of variation were obtained with a temperature
 439 combination of 2 °C and 28 °C as T_B and T_U thresholds, respectively. These temperatures
 440 are similar to those proposed by López-Bellido (1991) and Araya et al. (2010), and the
 441 same as those of Abrha et al. (2012) and López-Urrea et al. (2020). These results
 442 strengthen the values stipulated by the authors previously cited, whose studies were
 443 carried out under similar climatic conditions. The mean length of barley crop stages for
 444 CLM conditions are shown in Table 4.

445 Table 4. Length of barley growing stages in Castilla-La Mancha (accumulated GDD)
 446 according to development stages for MOPECO and AquaCrop models.

	MOPECO								AquaCrop		
	K _c (I)	K _c (II)	K _c (III)	K _c (IV)	K _y (i)	K _y (ii)	K _y (iii)	K _y (iv)	CnDv	MSsn	LSsn
Start	00	21	39	83	00	37	71	85	00	39	71
End	21	39	83	89	37	71	85	89	39	71	89
Average	290	744	1087	1450	645	981	1186	1450	715	949	1395
SD	46	57	64	69	73	64	59	69	66	71	68
CV (%)	16	8	6	5	11	7	5	5	9	7	5

447 where K_c (I): Initial; K_c (II): Crop development; K_c (III): Mid-season; K_c (IV): Late season; K_y (i):
 448 Vegetative period; K_y (ii): Flowering period; K_y (iii): Yield formation; K_y (iv): Ripening; CnDv: canopy
 449 development; MSsn: mid-season; LSsn: late season; 00: First day after sowing; 21: Beginning of tillering:
 450 first tiller detectable; 37: Flag leaf just visible, still rolled; 39: Flag leaf stage: flag leaf fully unrolled, ligule
 451 just visible; 71: Watery ripe: first grains have reached half their final size; 83: Early dough; 85: Soft dough:
 452 grain content soft but dry. Fingernail impression not held; 89: Fully ripe: grain hard, difficult to divide with
 453 thumbnail; SD: standard deviation; CV: coefficient of variation.

454 The methodologies used by both crop models, computing the required thermal time for
 455 reaching each development stages, showed similar values when the barley crop attained
 456 the same phenological stage (i.e. BBCH scales 39, 71 and 89), obtaining differences lower
 457 than 4.0%. In this sense, the accumulated GDD progression at the different crop growth
 458 stages (either those used by MOPECO or by AquaCrop) was similar in all monitored
 459 cropping seasons (Table A2, Annex), with the GDD variability decreasing (represented
 460 as coefficient of variation; Table 4) with time, as has also been observed by other authors
 461 using GDD (Lancaster et al., 1996; Marinaccio et al., 2015; Pereira et al., 2015; Piccinni
 462 et al., 2009; Ruiz-Corral et al., 2002). Analysing variability in days after sowing, there
 463 were differences in duration of between 2 and 11 days for the stages established by both
 464 crop models. These numbers of days represent, as a maximum, around 7% with respect
 465 to the total crop growth length (150 days). Thus, these variation results can be considered
 466 as acceptable, following the same criteria given by Domínguez et al. (2012c) in a maize
 467 crop cultivated in the same production area.

468 Finally, the average thermal time values calculated for the three main phenological stages
 469 used by the AquaCrop model (Table 4), were very similar to those calibrated by López-
 470 Urrea et al. (2020). These authors parameterized the conservative parameters “Time to
 471 maximum canopy cover” and “Length of the Harvest Index accumulation” as 619 GDD
 472 and 675 GDD, respectively. Taking into account that the crop canopy development stage

473 (CnDv) is the same as the first previous parameter described, CnDv was 13.4% higher.
474 This difference for the crop stage may be acceptable since the highest variations are
475 usually found in the first crop growth stage (Table 4). Conversely, the second
476 conservative parameter is represented as the GDD remainder between late-season (LSsn
477 (Table 4) and CnDv, obtaining 680 GDD, which is very close to the stage parameterized
478 by López-Urrea et al. (2020). Therefore, the average thermal time reported in Table 4 will
479 be used to simulate the crop cycle length under the conditions of $TMY_{intermediate}$.

480 **3.2. “Crop vs. irrigation water” production function obtained by the different** 481 **irrigation tools provided by the models**

482 The four irrigation strategies simulated by AquaCrop with a $TMY_{intermediate}$ reached a
483 maximum yield of $11.70 \times 10^3 \text{ kg ha}^{-1}$ (IS1_Aq, IS2_Aq, IS3_Aq and IS4_Aq; Table 2;
484 Fig. 3a). In the same way, and as expected, similar maximum yields were simulated by
485 MOPECO for the two irrigation strategies simulated (ORDI and ORDIL; Table 2; Fig.
486 3a). Although the MOPECO model was calibrated for a $Y_m = 9.00 \times 10^3 \text{ kg ha}^{-1}$ (Table
487 1), according to the results obtained in the experiments carried out by López-Urrea et al.
488 (2020), the Y_m is not a constant value and depends on many factors, such as climatic
489 conditions, soil characteristics and crop management (Sadras et al., 2015). Consequently,
490 this value must be adapted for the conditions of the farm and the year where the
491 simulations were or will be carried out. In this sense, and in order to achieve a proper
492 comparison between both models, the maximum yield obtained by AquaCrop was
493 considered as Y_m for MOPECO.

494 The barley yield simulated by using AquaCrop under rainfed conditions in a
495 $TMY_{intermediate}$ was $2.80 \times 10^3 \text{ kg ha}^{-1}$ (Table 2). This value, as well as the maximum
496 simulated yield can be considered appropriate, according to the crop statistics and field
497 trials carried out in this area (ITAP, 2020; MAPA, 2020). With respect to MOPECO, the
498 rainfed condition was not simulated since simulated yields are unreliable when the
499 computed ET_a/ET_m ratio for one or more development stages is lower than 0.5, as happens
500 under rainfed conditions (Domínguez et al., 2012a; Doorenbos and Kassam, 1979).

501 Overall, all ISs simulated by both models showed that the maximum yield was reached
502 when gross irrigation water depth (GIWD) was between 300 and 390 mm (Table 2; Fig.
503 3a). In the case of AquaCrop, and excepting IS1, all ISs simulated yields were close to
504 $11.70 \times 10^3 \text{ kg ha}^{-1}$ when GIWD was higher than 350 mm (Table 2), while slightly lower
505 GIWD values (ranging between 300 and 330 mm) decreased by yield around 12%. In
506 contrast, the two ISs simulated by MOPECO (ORDI and ORDIL) obtained the maximum
507 yield supplying 312 mm of GIWD (Table 2). Simulating GIWD lower than 300 mm, both
508 crop models showed that barley crop was subjected to water deficit (ET_a/ET_m ratio lower
509 than 1; Table 2). Nonetheless, all ISs simulated by MOPECO attained crop yields between
510 16% and 27% higher than those obtained by AquaCrop, considering similar GIWD
511 applications (Fig. 3a).

512 Analysing the IS simulated by AquaCrop, IS1, applying irrigation depths fixed at 23.5
513 mm per event, with an interval time between irrigation events of 1 to 7 days, showed that
514 is not feasible at either economic or environmental level. In this simulated interval time,
515 deep percolation was highly significant (between 88 and 2800 mm; Table 2), causing crop
516 yield not to increase significantly with a GIWD of more than 350 mm (Table 2; Fig. 3a).
517 Thus, IS1 simulated around 18% less crop yield for a GIWD interval between 300 and
518 390 mm. On the other hand, the irrigation scheduling managed by AquaCrop using the
519 readily available water in the soil (% RAW) as time criterion, showed that, depleting soil
520 water up to a 34 mm, and requiring GIWD between 330 and 490 mm, the simulated crop

521 yield was close to the maximum yield, obtaining ET_a/ET_m ratios of around 0.95 (Table
522 2), whereas with depletion thresholds higher than 34 mm or by fixing interval time
523 between irrigation events at more than 11 days, the AquaCrop model simulated
524 significant decreases in crop yield, with global ET_a/ET_m ratios lower than 0.85 (Table 2).
525 The AquaCrop results simulating high-frequency irrigation strategies (interval irrigation
526 events between 1 and 5 days or with a depletion threshold between 12 and 27 mm, IS2-
527 Aq and IS4-Aq, respectively), obtained average irrigation depths from 3 mm to 12 mm
528 per irrigation event (Table 2). These irrigation schedules are not useful, according to the
529 typical irrigation amount per event, although they attained the largest ET_a/ET_m ratios
530 ($>0.97\%$; Table 2). Finally, IS4-Aq also simulated irrigation scheduling with low
531 frequency of irrigation events (from 3 to 10 events along crop growth cycle; Table 2)
532 whose average irrigation depths per event were between 25% and 88% higher than the
533 objective irrigation water depth (23.5 mm), and consequently ET_a/ET_m ratios were lower
534 than 0.88 (Table 2).

535 Regarding the two ISs simulated by MOPECO, both showed that crop yield and ET_a/ET_m
536 ratio had a similar behaviour, since the GIWDs and MIWDs simulated in each case were
537 very close (Table 2), obtaining almost overlapping production function-curves (Fig. 3a).
538 Comparing the number of irrigation events simulated by both models, and under a similar
539 ET_a/ET_m ratio value, the strategies performed by MOPECO provided more frequent
540 irrigation events than AquaCrop. In the case of the simulated ET_a , and comparing data
541 with similar ET_a/ET_m ratios (Table 2), AquaCrop computed around 14% above MOPECO
542 because of the different method of calculating evapotranspiration.

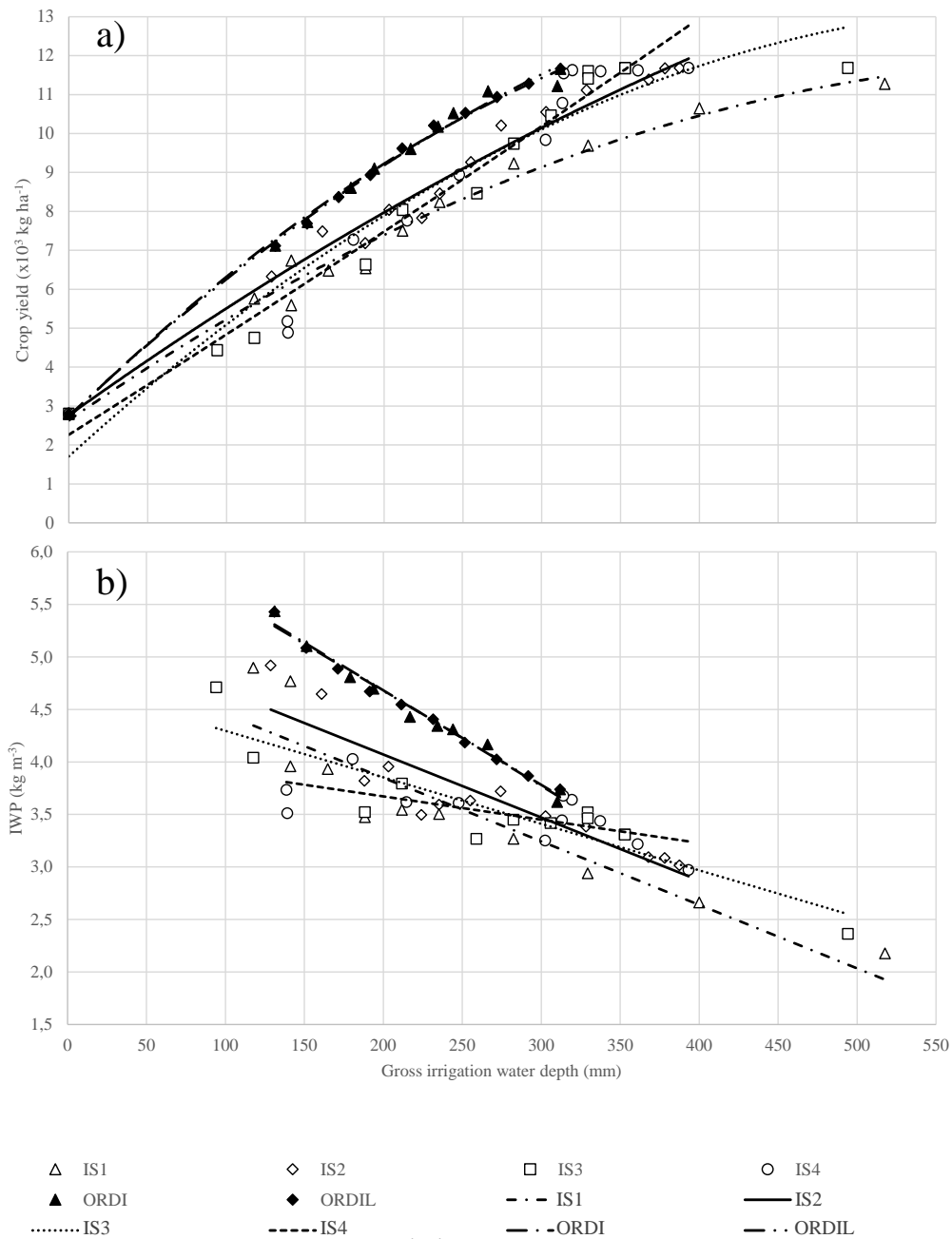
543 In general, the calculated IWP values ranged between 0.184 kg m^{-3} and 5.435 kg m^{-3}
544 (Table 2). The IWP simulated by AquaCrop showed a higher variability than MOPECO
545 (from 0.184 kg m^{-3} to 4.921 kg m^{-3} vs. from 3.619 kg m^{-3} to 5.435 kg m^{-3} , respectively;
546 Table 2, Fig. 3). Thus, the IWP differences for the four ISs simulated by AquaCrop were
547 significant, with GIWD lower than 200 mm (up to 20% less), while these differences
548 were between 9.5% and 15% with GIWD above 200 mm (Fig. 3b), excepting IS1, whose
549 calculated IWP tended to drop off significantly with respect to the rest of ISs (values
550 lower than 3.0 kg m^{-3} ; Fig. 3b). In contrast, the IWP computed by MOPECO had a similar
551 behaviour under the same GIWD (differences lower than 1.0%; Fig. 3b), as was also
552 shown with the simulated crop yield (Fig. 3a). Overall, the MOPECO model computed
553 higher IWP-GIWD relationships than those calculated by AquaCrop, being between 8.0%
554 and 27.5% on average when water deficit was triggered.

555 The production and IWP function curves obtained with MOPECO contained those
556 generated with AquaCrop (Fig. 3). The main reason for this is the way to outline the
557 different ISs, where the ISs considered for AquaCrop were sustained throughout the crop
558 cycle, whereas the ISs simulated by MOPECO established regulated irrigation
559 management based on the water deficit sensibility of each crop growth stage. Similar
560 differences between ORDI and sustained deficit irrigation (SDI) strategies were
561 computed by the MOPECO model, optimizing the deficit irrigation strategies for maize
562 in the same area (Domínguez et al., 2012a).

563 The models derived from the simulated ISs with both AquaCrop and MOPECO showed
564 that crop yield-water production functions had a high goodness of fit with the second-
565 degree polynomial model ($R^2 > 92\%$; Table A3, Annex), while IWP-GIWD relationships
566 for all ISs were faithfully fitted to a linear model (Table A3, Annex). The selected
567 curvilinear model, as well as their parameter values for each IS, were, in most cases,
568 highly significant, with standard errors of the model ranging between 0.17×10^3 and 0.85
569 $\times 10^3 \text{ kg ha}^{-1}$ (Table A3, Annex), where the ISs generated by AquaCrop simulated a 67%

570 larger standard error than MOPECO. In the case of linear models, errors were around 0.01
571 kg m⁻³ for the ISs simulated by MOPECO and between 0.06 kg m⁻³ and 0.19 kg m⁻³ for
572 those generated with AquaCrop (Fig. 3b). Finally, the curvilinear model adjusted to IS4
573 showed that the squared term had no significance, being a linear relationship that would
574 achieve highly significant model coefficients. Trout and DeJonge (2017), in a field trial
575 with maize during four cropping seasons, derived consistent and highly significant fits of
576 crop-water production functions to a curvilinear model. These authors, relating crop yield
577 vs. evapotranspiration with the former model, obtained similar results, despite several
578 studies having projected linear relationships in field crops (Doorenbos and Kassam, 1979;
579 Fereres and Soriano, 2007; Saseendran et al., 2015; Steduto et al., 2007; Tanner and
580 Siinclair, 1983). In this sense, reasons such as evaporation losses decreasing as water
581 deficit limits transpiration could partly explain those results (Trout and DeJonge, 2017).

582



583 Figure 3. Relationships between barley yield and gross irrigation water depth (GIWD) (a), and irrigation
 584 water productivity and GIWD (b) simulated by both AquaCrop (white symbols) and MOPECO (black
 585 symbols) models.

586 **3.3. Simulation by AquaCrop of the data from the ORDIL experimental field tests,**
587 **validation of the results, and comparison with MOPECO outputs**

588 Overall, the AquaCrop model performance simulating the irrigation scheduling derived
589 from different ORDIL levels was appropriate during the three experimental seasons. The
590 progression of the main crop growth variables simulated by AquaCrop (canopy cover,
591 CC; aboveground biomass, AGB), as well as final crop yield (Y) followed a tendency
592 close to the measured data (Fig. 4; Table 5). The calculated statistical indicators between
593 observed and simulated data showed that CC was underestimated with MBE values
594 between 0.6% and 7.1%, and whose variance of error values were around 11.0% for all
595 treatments (Table 5). Most values of EF and d were close to 0.90 or higher, excepting two
596 treatments during the 2016 cropping season (80% and 70%; Table 5), showing that
597 AquaCrop had a good goodness of fit. This slight underestimation of the CC by AquaCrop
598 also resulted in the same trend at that of the measured AGB data (Fig. 4), reporting errors
599 ranging from 0.76×10^3 to 2.17×10^3 kg ha⁻¹ (Table 5). Finally, goodness of fit indicators
600 were similar to those computed for CC in this research.

601 With respect to the simulated crop yield, AquaCrop simulated values close to those
602 observed, including the standard deviation values (Table 5). Thus, the percentage of
603 deviation between both simulated and observed values, for all treatments, was within
604 $\pm 10\%$ (Table 5); obtaining errors between 0.26×10^3 and 0.46×10^3 kg ha⁻¹ with high EF
605 and d values (Table 5). The crop yield statistical indicators computed, between the data
606 simulated by MOPECO vs. the observed data, showed similar results to those obtained
607 with AquaCrop, with the RMSE values being somewhat lower (Table 5). Pardo et al.
608 (2020) extensively discussed testing the MOPECO model with the ORDIL methodology,
609 concluding that Y_m is the most important variable to fit the potential crop yield to the
610 actual yield, according to phenological stage duration, suitable parameterization of K_c and
611 K_y and optimal volume water distribution along the crop cycle, depending on the actual
612 weather conditions.

613 Comparing the former results with those reported by López-Urrea et al. (2020), who
614 parameterized this model for barley under the same climate conditions, it is worth noting
615 that all statistical parameters used to test both models were similar. Thus, these findings
616 confirm the suitability of barley parameterization in AquaCrop and MOPECO and, in
617 addition, the different irrigation strategies developed by ORDIL methodology, and tested
618 in the field, were faithfully replicated by the models.

619 In terms of evaporative demand simulated by both models, the accumulated maximum
620 and actual crop evapotranspiration (ET_m and ET_a, respectively) simulated by AquaCrop
621 were, respectively, around 17% and 8% higher than those obtained by MOPECO (Table
622 6). In this sense, both the total actual crop transpiration (T_a) and the total actual soil
623 evaporation (E_a) values simulated by AquaCrop were not satisfied in any irrigation
624 treatment without water deficit (i.e. ND and 100% over 2500) during the three seasons
625 (Table 6). However, the ET_a/ET_m ratio values calculated by MOPECO for ND treatment
626 were fully satisfied, excepting the second experimental season with 0.96 (Table 6). In this
627 sense, López-Urrea et al. (2020) reported differences in the ET_a and ET_m simulated by
628 the models. This research shows again that as water levels are reduced, the differences in
629 simulated ET_a and ET_m across crop models are larger (mean values from 4% and 15% for
630 ND to 11% and 20% for 70%, respectively; Table 6). The main factors that might explain
631 these differences are:

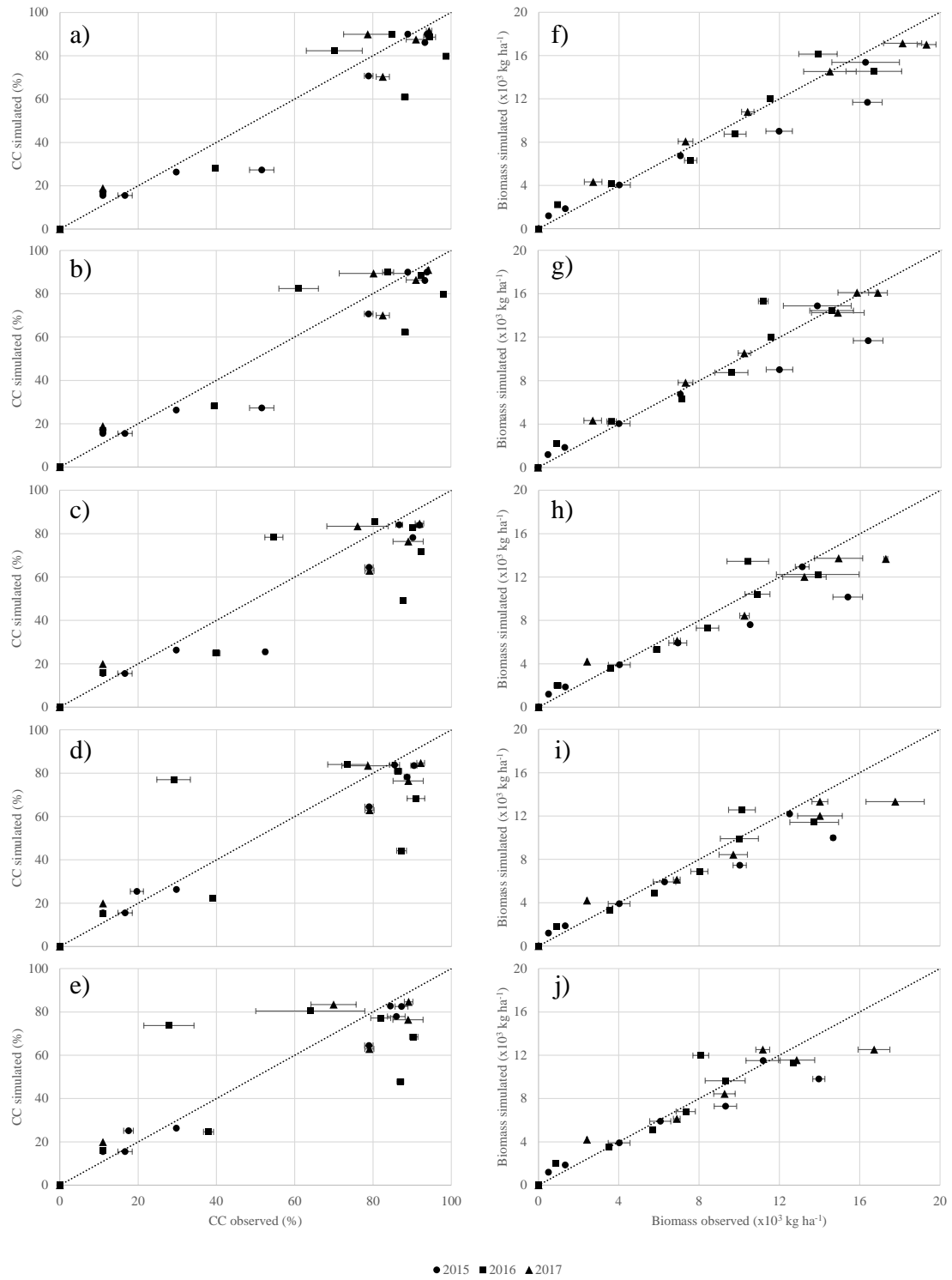
- 632 - The single and dual K_c approaches coded in MOPECO and AquaCrop models,
633 respectively. The ET_a/ET_m ratio simulated for ND treatment by MOPECO was

634 almost matched in the three seasons (≈ 1.0 ; Table 6), while AquaCrop failed to
635 reach ratios higher than 0.85% because of the low simulated actual evaporation,
636 since actual transpiration was close to the maximum (Table 6).

637 - Runoff. The simulation of this variable by both models showed large differences,
638 being between 76% and 190% lower for AquaCrop. If the AquaCrop model
639 considered the same water outtake by runoff as MOPECO, the ET_a/ET_m ratio
640 simulated by both models would be reduced from 12% to 8% as the mean value,
641 for the three seasons (Table 7).

642 - Updating K_{cb} barley. Pereira et al., (2021b) updated the basal crop coefficient
643 (K_{cb}) of field crops, such as grain legumes, oil crops and small grain cereals. In
644 this case, K_{cb} for barley was determined as 1.00. Changing this value in the crop
645 transpiration coefficient ($K_{CTR}=1.10$; Table 1), and simulating once again all
646 treatments, the new mean differences in ET_a/ET_m ratio between the two models
647 were around 8% (Table 7); attaining 4% mean difference when the same runoff
648 value was considered (Table 7). This change in K_{CTR} value did not generate a
649 lower simulated yield for the different treatments, obtaining mean differences of
650 around 1% (Table 7). Therefore, this sensitivity analysis on modifying K_{CTR} for
651 AquaCrop, would allow differences in ET_a/ET_m ratios between the two crop
652 models to be reduced without significant effects on simulating crop yield and
653 being close to the actual yield data.

654 Finally, Pohanková et al. (2018), testing the performance of several crop models with
655 spring barley, simulated cumulative ET_a from sowing to maturity with AquaCrop
656 between 350 and 400 mm in three locations of Czech Republic. Although both climate
657 conditions and the crop cycle lengths (given in days) are different to those in this research,
658 the ET_a simulated by these authors were similar to those shown in Table 6. In addition,
659 they calculated the actual crop Transpiration (T_a) as 78% of ET_a on average, being close
660 to values found in the present paper (around 75% for AquaCrop).



661 Figure 4. Comparison between observed canopy cover (a-e) and aboveground biomass (f-j) data vs. those
 662 simulated by AquaCrop during the three experimental seasons for the five ORDI treatments (ND: a and f;
 663 100%: b and g; 90%: c and h; 80%: d and i; 70%: e and j). The dashed line shows a 1:1 function.

664

665 Table 5. Statistical indicators obtained for yield at harvest with AquaCrop and MOPECO models, and both canopy cover and above ground biomass
 666 evolution with AquaCrop.

E.Y.	Treat.	Yield at harvest*														Canopy cover ^{&}				Above ground biomass ^{&}									
		Obs. (x 10 ³ kg ha ⁻¹)		Sim. (x 10 ³ kg ha ⁻¹)		Dev. (%)		n	RMSE (x 10 ³ kg ha ⁻¹)		MBE (x 10 ³ kg ha ⁻¹)		EF		d		n	RMSE (%)	MBE (%)	EF	d	n	RMSE (x10 ³ kg ha ⁻¹)	MBE (x10 ³ kg ha ⁻¹)	EF	d			
		Aq	MO	Aq	MO	Aq	MO		Aq	MO	Aq	MO	Aq	MO	Aq	MO													
2015	ND	9.199 (0.619) [#]	9.465	8.936	-	2.89	2.86										9	9.2	-4.8	0.93	0.98	8	2.021	-	0.956	0.90	0.97		
	100%	8.616 (0.457)	9.007	8.496	-	4.54	1.39										9	9.2	-4.8	0.93	0.98	8	2.028	-	0.713	0.89	0.97		
	90%	7.620 (0.362)	7.525	7.667	-	1.25	0.62	5	0.339	0.172	0.021	-	0.071	0.92	0.97	0.98	0.99	9	11.5	-7.1	0.89	0.97	8	2.168	-	1.025	0.85	0.95	
	80%	7.367 (0.169)	6.788	7.174	7.87	3.43												9	7.0	-3.1	0.96	0.99	8	1.922	-	0.850	0.87	0.96	
	70%	6.404 (0.492)	6.316	6.569	1.38	-	2.57											9	6.6	-2.4	0.96	0.99	8	1.668	-	0.613	0.88	0.96	
2016	ND	8.877 (0.296)	9.728	8.647	-	9.59	2.59										9	12.8	-4.6	0.89	0.97	8	1.344	-	0.013	0.94	0.99		
	100%	7.985 (0.301)	8.533	7.250	-	6.86	9.21										9	13.7	-2.9	0.87	0.97	8	1.612	-	0.593	0.90	0.98		
	90%	7.690 (0.444)	7.709	7.239	-	0.25	5.86	5	0.463	0.450	-	-	0.290	0.398	0.83	0.71	0.95	0.93	9	17.6	-5.3	0.78	0.94	8	1.363	-	0.032	0.91	0.98
	80%	7.214 (0.215)	7.085	6.758	1.79	6.32												9	23.8	-2.8	0.57	0.88	8	1.333	-	0.163	0.91	0.98	
	70%	6.331 (0.148)	6.486	6.211	-	2.45	1.89											9	22.6	-1.3	0.58	0.88	8	1.540	-	0.361	0.85	0.96	
2017	ND	9.071 (0.511)	9.057	8.994	0.16	0.85											6	7.7	0.0	0.96	0.99	7	1.174	-	0.079	0.97	0.99		
	100%	8.032 (0.398)	8.088	7.684	-	0.69	4.33										6	7.5	-0.6	0.96	0.99	7	0.759	-	0.181	0.98	1.00		
	90%	7.621 (0.250)	8.073	7.350	-	5.93	3.56	5	0.256	0.253	-	-	0.194	0.218	0.91	0.92	0.98	0.98	6	10.0	-3.3	0.93	0.98	7	1.809	-	0.969	0.91	0.97
	80%	7.311 (0.232)	7.606	6.966	-	4.03	4.72											6	9.8	-3.8	0.93	0.98	7	2.058	-	1.052	0.88	0.96	
	70%	6.283 (0.295)	6.464	6.230	-	2.88	0.84										6	10.8	-1.8	0.91	0.98	7	1.912	-	0.562	0.88	0.96		

667 E.Y.: experimental year; Treat.: treatment; *: yield performed against yield commercial grain (12% of water content); &: statistical indicators obtained from the simulated values with AquaCrop
 668 model; #: values between brackets are the standard deviation; Obs.: observed; Sim.: simulated; Aq: AquaCrop; MO: MOPECO; Dev.: deviation; n: number of data point; RMSE: root mean square
 669 error; MBE: mean bias error; EF: model efficiency; d: Willmot's index of agreement.

670

671 Table 6. Comparison of the evapotranspiration and runoff values simulated by AquaCrop and MOPECO models for the three experimental seasons.

E.Y.	Treat.	Aq. variables			Sim. ET _a (mm)			Sim. ET _m (mm)			Sim. ET _a /ET _m (%)			Sim. runoff (mm)		
		T _a (mm)	T _a /T _m (%)	E _a /E _m (%)	Aq	MO	Dif. Aq-MO	Aq	MO	Dif. Aq-MO	Aq	MO	Dif. Aq-MO	Aq	MO	Dif. Aq-MO
2015	ND	335.9	96	72	422.1	386.2	9	498.2	387.7	22	85	100	-18	11.9	25.1	-111
	100%	320.6	93	68	401.4	364.3	9	498.2	387.7	22	81	94	-17	11.9	25.1	-111
	90%	281.2	88	68	375.6	332.3	12	497.8	380.7	24	75	87	-16	12.4	25.1	-102
	80%	259.5	85	67	354.4	309.6	13	497.9	376.5	24	71	82	-16	12.4	25.1	-102
	70%	240.5	83	63	330.5	284.0	14	497.7	372.4	25	66	76	-15	12.0	25.1	-109
2016	ND	319.0	94	79	427.1	417.3	2	494.0	433.4	12	86	96	-11	14.0	24.7	-76
	100%	290.7	86	74	386.2	360.3	7	494.0	428.8	13	78	84	-7	14.1	26.3	-87
	90%	259.6	84	73	366.9	354.1	3	493.8	427.8	13	74	83	-11	8.9	0.0	100
	80%	240.5	82	70	344.1	325.0	6	492.3	414.3	16	70	78	-12	6.8	0.0	100
	70%	220.2	78	67	323.9	302.5	7	493.7	414.3	16	66	73	-11	6.7	0.0	100
2017	ND	355.3	98	79	455.2	448.5	1	506.8	448.8	11	90	100	-11	26.4	68.9	-161
	100%	324.9	91	68	399.8	375.3	6	506.9	443.5	13	79	85	-7	22.3	64.6	-190
	90%	278.0	87	70	375.3	360.1	4	506.3	446.9	12	74	81	-9	22.3	52.0	-133
	80%	264.7	84	69	360.2	326.0	9	506.3	423.4	16	71	77	-8	22.4	45.8	-104
	70%	239.7	81	69	335.5	293.8	12	506.3	415.6	18	66	71	-7	22.7	44.4	-96

E.Y.: experimental year; Treat.: treatment; Tw: total water received (mm); I: gross irrigation; Aq.: AquaCrop; MO: MOPECO; Sim.: simulated; ET_a: actual evapotranspiration; ET_m: maximum evapotranspiration; T_a: actual transpiration; T_m: maximum transpiration; E_a: actual evaporation; E_m: maximum evaporation; Dif.: difference in %.

672

673

674

675

676

677

678 Table 7. Sensibility analysis of the ET_a/ET_m ratios simulated by AquaCrop and MOPECO models during three experimental seasons using the
 679 same runoff considered by MOPECO.

E.Y.	Treat.	Sim. ET_a/ET_m (%) ¹			Sim. ET_a/ET_m (%) ²			Sim. ET_a/ET_m (%) ³			Crop yield ($\times 10^3$ kg ha ⁻¹) ⁴		
		Aq	MO	Dif. Aq-MO	Aq	MO	Dif. Aq-MO	Aq	MO	Dif. Aq-MO	Aq ($K_{CTR}=1.00$)	Aq ($K_{CTR}=1.10$)	Dif.
2015	ND	87	100	-14	85	100	-17	88	100	-14	8.940	9.465	-6
	100%	83	94	-14	83	94	-13	85	94	-10	8.776	9.007	-3
	90%	77	87	-13	79	87	-10	81	87	-7	7.627	7.525	1
	80%	73	82	-13	75	82	-9	77	82	-6	7.044	6.788	4
	70%	68	76	-12	70	76	-8	72	76	-5	6.566	6.316	4
2016	ND	88	96	-9	88	96	-10	90	96	-7	9.241	9.728	-5
	100%	80	84	-5	80	84	-4	83	84	-2	8.403	8.533	-3
	90%	73	83	-13	78	83	-6	76	83	-9	7.660	7.709	-1
	80%	69	78	-14	73	78	-7	72	78	-9	7.091	7.085	0
	70%	65	73	-13	69	73	-5	68	73	-7	6.663	6.486	3
2017	ND	98	100	-2	90	100	-10	99	100	-1	8.501	9.057	-6
	100%	86	85	2	81	85	-5	88	85	4	7.810	8.088	-3
	90%	79	81	-2	76	81	-6	81	81	1	7.861	8.073	-2
	80%	75	77	-3	75	77	-3	79	77	2	7.639	7.606	1
	70%	69	71	-3	71	71	0	74	71	4	6.722	6.464	4

E.Y.: experimental year; Treat.: treatment; Sim.: simulated; ET_a : actual evapotranspiration; ET_m : maximum evapotranspiration; ¹: Simulating treatments with the same runoff value computed by MOPECO; ²: simulating treatments with $K_{CTR}=1.00$; ³: simulating treatments with $K_{CTR}=1.00$ and considering the same runoff value as MOPECO; ⁴: crop yield (12% of water content) simulated by AquaCrop changing the K_{CTR} value and equal runoff value than MOPECO; Aq: AquaCrop; MO: MOPECO; Dif.: difference in %.

680

681

682 4. Conclusions

683 The AquaCrop and MOPECO models can be used to evaluate the effect of various
684 irrigation schedules on crop yield and the water productivity response, given that, when
685 both are well calibrated, they show no differences. The results obtained by the AquaCrop
686 model allowed us to compare its performance with a larger number of measured barley
687 growth variables (aboveground biomass, canopy cover and crop yield) than MOPECO
688 (only crop yield). To generate these results, AquaCrop requires a large number of
689 parameters, making its management somewhat more difficult than MOPECO. The range
690 of simulations obtained by AquaCrop is higher than MOPECO, since, under semiarid
691 conditions, it is able to simulate rainfed crop growth. Thus, when the accumulated
692 ET_a/ET_m ratio is lower than 0.5 in one or more crop growth stages, MOPECO's results
693 may not be suitable.

694 Although AquaCrop software has different options for building an automatic schedule
695 irrigation, the optimized irrigation scheduling based on ORDI and ORDIL
696 methodologies, provided by MOPECO, attained significant irrigation water productivity
697 (IWP). Thus, considering the hypothesis of this research, the IWP simulated by MOPECO
698 was between 8.0% and 28.0% higher than AquaCrop, with different irrigation water
699 amounts applied to the crop. Therefore, if MOPECO is properly parameterized, this
700 methodology can be of great help in establishing irrigation scheduling in areas with
701 limited water resources to improve the IWP. Conversely, AquaCrop users must be
702 sufficiently qualified to plan an irrigation strategy whose IWP levels can be similar than
703 those reached by MOPECO, especially under deficit irrigation conditions.

704 The effects of four irrigation strategies proposed by ORDIL methodology in both canopy
705 cover and aboveground biomass evolution, as well as the final yield of barley crop during
706 three-field seasons were appropriately simulated by AquaCrop. Therefore, the water
707 deficit levels established by ORDIL for each crop barley development stage were in
708 suitable ranges for simulating this crop with AquaCrop. Finally, we consider that a
709 combination of both crop models may be especially interesting for analysis of the crop's
710 physiological behaviour in response to an optimized deficit irrigation strategy coded by
711 MOPECO. Nevertheless, soil evaporation and crop transpiration data should be used with
712 caution given the differences in findings between the crop models.

713

714 Acknowledgements

715 This paper was developed within the framework of the project AGL2017-82927-C3-3-R
716 funded by the Spanish Ministry of Economy, Industry and Competitiveness, together with
717 FEDER funds.

718

719 References

- 720 Abbrha, B., Delbecque, N., Raes, D., Tsegay, A., Todorovic, M., Heng, L., Vanutrecht, E.,
721 Geerts, S., Garcia-Vila, M., Deckers, S., 2012. Sowing strategies for barley
722 (*Hordeum vulgare* L.) based on modelled yield response to water with Aquacrop.
723 *Exp. Agric.* 48, 252–271. <https://doi.org/10.1017/S0014479711001190>
- 724 Acevedo, E., Silva, P., Silva, H., 2002. Wheat growth and physiology, in: Curtis, B.,
725 Rajaram, S., Gómez Macpherson, H. (Eds.), *Bread Wheat, Improvement and*
726 *Production*. FAO Plant Production and Protection Series, p. 30.

- 727 Allen, R., Pereira, L., Raes, D., Smith, M., 1998. Crop Evapotranspiration-Guidelines for
728 Computing Crop Water Requirements, FAO. ed. FAO Irrigation and Drainage Paper
729 56., Rome, Italy.
- 730 Araya, A., Habtu, S., Hadgu, K.M., Kebede, A., Dejene, T., 2010. Test of AquaCrop
731 model in simulating biomass and yield of water deficient and irrigated barley
732 (*Hordeum vulgare*). *Agric. Water Manag.* 97, 1838–1846.
733 <https://doi.org/10.1016/j.agwat.2010.06.021>
- 734 Bleiholder, H., Weber, E., Lancashire, P., Feller, C., Buhr, L., Hess, M., Wicke, H., Hack,
735 H., Meier, U., Klose, R., van den Boom, T., Stauss, R., 2001. Growth Stages of
736 Mono-and Dicotyledonous Plants BBCH Monograph. Braunschweig, Germany.
- 737 CHG, 2020. Plan Hidrológico de cuenca [WWW Document]. Confed. Hidrográfica del
738 Guadiana. URL [https://www.chguadiana.es/planificacion/plan-hidrologico-de-la-](https://www.chguadiana.es/planificacion/plan-hidrologico-de-la-demarcacion/ciclo-de-planificacion-2015-2021-vigente/Introduccion)
739 [demarcacion/ciclo-de-planificacion-2015-2021-vigente/Introduccion](https://www.chguadiana.es/planificacion/plan-hidrologico-de-la-demarcacion/ciclo-de-planificacion-2015-2021-vigente/Introduccion) (accessed
740 6.5.20).
- 741 CHJ, 2020. Plan Hidrológico de cuenca [WWW Document]. Confed. Hidrográfica del
742 Júcar. URL [https://www.chj.es/es-](https://www.chj.es/es-es/Organismo/normativa/Paginas/Normativa.aspx)
743 [es/Organismo/normativa/Paginas/Normativa.aspx](https://www.chj.es/es-es/Organismo/normativa/Paginas/Normativa.aspx) (accessed 6.5.20).
- 744 Cossani, C.M., Slafer, G.A., Savin, R., 2009. Yield and biomass in wheat and barley
745 under a range of conditions in a Mediterranean site. *F. Crop. Res.* 112, 205–213.
746 <https://doi.org/10.1016/j.fcr.2009.03.003>
- 747 Cramer, W., Guiot, J., Marini, K., Azzopardi, B., Balzan, M., Cherif, S., Doblaz-Miranda,
748 E., dos Santos, M., Drobinski, P., Fader, M., El Rahman, A., Giupponi, C., Koubi,
749 V., Lange, M., Lionello, P., Llasat, M., Moncada, S., Mrabet, R., Paz, S., Savé, R.,
750 Snoussi, M., Toreti, A., Vafeidis, A.T., Xoplaki, E., 2020. MedECC 2020 Summary
751 for Policymakers., in: Cramer, W., Guiot, J., Marini, K. (Eds.), *Climate and*
752 *Environmental Change in the Mediterranean Basin – Current Situation and Risks for*
753 *the Future. First Mediterranean Assessment Report. Union for the Mediterranean,*
754 *Plan Bleu, UNEP/MAP, Marseille, France, p. 34.*
- 755 De Juan, J.A., Tarjuelo, J.M., Valiente, M., García, P., 1996. Model for optimal cropping
756 patterns within the farm based on crop water production functions and irrigation
757 uniformity. I: Development of a decision model. *Agric. Water Manag.* 31, 115–143.
758 [https://doi.org/10.1016/0378-3774\(95\)01219-2](https://doi.org/10.1016/0378-3774(95)01219-2)
- 759 de Wit, A., Boogaard, H., Fumagalli, D., Janssen, S., Knapen, R., van Kraalingen, D.,
760 Supit, I., van der Wijngaart, R., van Diepen, K., 2019. 25 years of the WOFOST
761 cropping systems model. *Agric. Syst.* 168, 154–167.
762 <https://doi.org/10.1016/j.agsy.2018.06.018>
- 763 Domínguez-Niño, J.M., Oliver-Manera, J., Girona, J., Casadesús, J., 2020. Differential
764 irrigation scheduling by an automated algorithm of water balance tuned by
765 capacitance-type soil moisture sensors. *Agric. Water Manag.* 228, 105880.
766 <https://doi.org/10.1016/j.agwat.2019.105880>
- 767 Domínguez, A., De Juan, J., 2008. Agricultural water management in Castilla-La Mancha
768 (Spain), in: Sorensen, M. (Ed.), *Agricultural Water Management Research Trends.*
769 Nova Science Publishers, Inc., New York, USA, pp. 99–128.
- 770 Domínguez, A., de Juan, J.A., Tarjuelo, J.M., Martínez, R.S., Martínez-Romero, A.,
771 2012a. Determination of optimal regulated deficit irrigation strategies for maize in a

772 semi-arid environment. *Agric. Water Manag.* 110, 67–77.
773 <https://doi.org/10.1016/j.agwat.2012.04.002>

774 Domínguez, A., Jiménez, M., Tarjuelo, J.M., de Juan, J.A., Martínez-Romero, A., Leite,
775 K.N., 2012b. Simulation of onion crop behavior under optimized regulated deficit
776 irrigation using MOPECO model in a semi-arid environment. *Agric. Water Manag.*
777 113, 64–75. <https://doi.org/10.1016/j.agwat.2012.06.019>

778 Domínguez, A., Martínez-Romero, A., Leite, K.N., Tarjuelo, J.M., de Juan, J.A., López-
779 Urrea, R., 2013. Combination of typical meteorological year with regulated deficit
780 irrigation to improve the profitability of garlic growing in central Spain. *Agric. Water*
781 *Manag.* 130, 154–167. <https://doi.org/10.1016/j.agwat.2013.08.024>

782 Domínguez, A., Martínez, R.S., De Juan, J.A., Martínez-Romero, A., Tarjuelo, J.M.,
783 2012c. Simulation of maize crop behavior under deficit irrigation using MOPECO
784 model in a semi-arid environment. *Agric. Water Manag.* 107, 42–53.
785 <https://doi.org/10.1016/j.agwat.2012.01.006>

786 Domínguez, A., Tarjuelo, J.M., de Juan, J.A., López-Mata, E., Breidy, J., Karam, F.,
787 2011. Deficit irrigation under water stress and salinity conditions: The MOPECO-
788 Salt Model. *Agric. Water Manag.* 98, 1451–1461.
789 <https://doi.org/10.1016/j.agwat.2011.04.015>

790 Doorenbos, J., Kassam, A., 1979. Yield Response to Water. Irrigation and Drainage Paper
791 No. 33. FAO, Rome, Italy.

792 FAOSTAT, 2019. Food and Agriculture Organization of the United Nations. Statistic
793 Division. [WWW Document]. URL <http://www.fao.org/faostat/en/#home> (accessed
794 11.24.19).

795 Farahani, H.J., Izzi, G., Oweis, T.Y., 2009. Parameterization and evaluation of the
796 aquacrop model for full and deficit irrigated cotton. *Agron. J.* 101, 469–476.
797 <https://doi.org/10.2134/agronj2008.0182s>

798 Fereres, E., Soriano, M.A., 2007. Deficit irrigation for reducing agricultural water use. *J.*
799 *Exp. Bot.* 58, 147–159. <https://doi.org/10.1093/jxb/erl165>

800 Foster, T., Brozović, N., Butler, A.P., Neale, C.M.U., Raes, D., Steduto, P., Fereres, E.,
801 Hsiao, T.C., 2017. AquaCrop-OS: An open source version of FAO's crop water
802 productivity model. *Agric. Water Manag.* 181, 18–22.
803 <https://doi.org/10.1016/j.agwat.2016.11.015>

804 García, I.F., Lecina, S., Ruiz-Sánchez, M.C., Vera, J., Conejero, W., Conesa, M.R.,
805 Domínguez, A., Pardo, J.J., Lélis, B.C., Montesinos, P., 2020. Trends and
806 challenges in irrigation scheduling in the semi-arid area of Spain. *Water*
807 (Switzerland) 12, 1–26. <https://doi.org/10.3390/w12030785>

808 Giunta, F., Motzo, R., Deidda, M., 1993. Effect of drought on yield and yield components
809 of durum wheat and triticale in a Mediterranean environment. *F. Crop. Res.* 33, 399–
810 409. [https://doi.org/10.1016/0378-4290\(93\)90161-F](https://doi.org/10.1016/0378-4290(93)90161-F)

811 Heng, L.K., Hsiao, T., Evett, S., Howell, T., Steduto, P., 2009. Validating the FAO
812 aquacrop model for irrigated and water deficient field maize. *Agron. J.* 101, 488–
813 498. <https://doi.org/10.2134/agronj2008.0029xs>

814 ITAP, 2020. Ensayos de CEREALES y COLZA. Boletín nº 101 8.

815 JCRMO, 2020. Normas de gestión, coordinación y control de los aprovechamientos de

- 816 regadío de la Mancha Oriental para la campaña de riegos 2019-2020. Albacete,
817 Spain.
- 818 Juskiw, P., Jame, Y., Kryzanowski, L., 2001. Phenological development of spring barley
819 in a short-season growing area. *Agron. J.* 93, 370–379.
- 820 Kloss, S., Pushpalatha, R., Kamoyo, K.J., Schütze, N., 2012. Evaluation of crop models
821 for simulating and optimizing deficit irrigation systems in arid and semi-arid
822 countries under climate variability. *Water Resour. Manag.* 26, 997–1014.
823 <https://doi.org/10.1007/s11269-011-9906-y>
- 824 Kuschel-Otárola, M., Rivera, D., Holzapfel, E., Palma, C.D., Godoy-Faúndez, A., 2018.
825 Multiperiod optimisation of irrigated crops under different conditions of water
826 availability. *Water (Switzerland)* 10, 1–23. <https://doi.org/10.3390/w10101434>
- 827 Lancaster, J., Triggs, C., DeRuijter, J., Gandar, P., 1996. Bulbing in onions: photoperiod
828 and temperature requirements and prediction of bulb size and maturity. *Ann. Bot.*
829 78, 423–430.
- 830 Leite, K.N., Martínez-Romero, A., Tarjuelo, J.M., Domínguez, A., 2015. Distribution of
831 limited irrigation water based on optimized regulated deficit irrigation and typical
832 meteorological year concepts. *Agric. Water Manag.* 148, 164–176.
833 <https://doi.org/10.1016/j.agwat.2014.10.002>
- 834 López-Bellido, L., 1991. *Cultivos Herbáceos Extensivos. Cereales.* Ediciones Mundi-
835 Prensa, Madrid, Spain.
- 836 López-Mata, E., Orengo-Valverde, J.J., Tarjuelo, J.M., Martínez-Romero, A.,
837 Domínguez, A., 2016. Development of a direct-solution algorithm for determining
838 the optimal crop planning of farms using deficit irrigation. *Agric. Water Manag.* 171,
839 173–187. <https://doi.org/10.1016/j.agwat.2016.03.015>
- 840 López-Mata, E., Tarjuelo, J.M., de Juan, J.A., Ballesteros, R., Domínguez, A., 2010.
841 Effect of irrigation uniformity on the profitability of crops. *Agric. Water Manag.* 98,
842 190–198. <https://doi.org/10.1016/j.agwat.2010.08.006>
- 843 López-Urrea, R., Domínguez, A., Pardo, J.J., Montoya, F., García-Vila, M., Martínez-
844 Romero, A., 2020. Parameterization and comparison of the AquaCrop and
845 MOPECO models for a high-yielding barley cultivar under different irrigation
846 levels. *Agric. Water Manag.* 230, 105931.
847 <https://doi.org/10.1016/j.agwat.2019.105931>
- 848 Lorite, I.J., García-Vila, M., Santos, C., Ruiz-Ramos, M., Fereres, E., 2013. AquaData
849 and AquaGIS: Two computer utilities for temporal and spatial simulations of water-
850 limited yield with AquaCrop. *Comput. Electron. Agric.* 96, 227–237.
851 <https://doi.org/10.1016/j.compag.2013.05.010>
- 852 MAPA, 2020. Anuario de Estadística 2019 [WWW Document]. Minist. Agric. Pesca y
853 Aliment. URL
854 [https://www.mapa.gob.es/es/estadistica/temas/publicaciones/anuario-de-](https://www.mapa.gob.es/es/estadistica/temas/publicaciones/anuario-de-estadistica/default.aspx)
855 [estadistica/default.aspx](https://www.mapa.gob.es/es/estadistica/temas/publicaciones/anuario-de-estadistica/default.aspx) (accessed 9.20.20).
- 856 Marinaccio, F., Reyneri, A., Blandino, M., 2015. Enhancing grain yield and quality of
857 winter barley through agronomic strategies to prolong canopy greenness. *F. Crop.*
858 *Res.* 170, 109–118.
- 859 Martínez-Romero, A., Domínguez, A., Landeras, G., 2019. Regulated deficit irrigation
860 strategies for different potato cultivars under continental Mediterranean-Atlantic

861 conditions. *Agric. Water Manag.* 216, 164–176.
862 <https://doi.org/10.1016/j.agwat.2019.01.030>

863 McMaster, G., Wilhelm, W., 1997. Growing degree-days: one equation, two
864 interpretations. *Agric. For. Meteorol.* 87, 291–300.

865 Microsoft, C., 2018. Microsoft Excel.

866 Ortega Álvarez, J.F., De Juan Valero, J.A., Tarjuelo Martín-Benito, J.M., López Mata,
867 E., 2004. MOPECO: An economic optimization model for irrigation water
868 management. *Irrig. Sci.* 23, 61–75. <https://doi.org/10.1007/s00271-004-0094-x>

869 Pardo, J.J., Martínez-Romero, A., Lélis, B.C., Tarjuelo, J.M., Domínguez, A., 2020.
870 Effect of the optimized regulated deficit irrigation methodology on water use in
871 barley under semiarid conditions. *Agric. Water Manag.* 228, 105925.
872 <https://doi.org/10.1016/j.agwat.2019.105925>

873 Pereira, L., Paredes, P., Rodrigues, G., Neves, M., 2015. Modeling barley water use and
874 evapotranspiration partitioning in two contrasting rainfall years. Assessing
875 SIMDualKc and AquaCrop models. *Agric. Water Manag.* 159, 239–254.

876 Pereira, L., Teodoro, P., Rodrigues, P., Teixeira, J., 2003. Irrigation Scheduling
877 Simulation: The Model Isareg, in: Rossi, G., Cancelliere, A., Pereira, L., Oweis, T.,
878 Shatanawi, M., Zairi, A. (Eds.), *Tools for Drought Mitigation in Mediterranean*
879 *Regions*. Springer, Dordrecht. https://doi.org/10.1007/978-94-010-0129-8_10

881 Pereira, L.S., Paredes, P., Hunsaker, D.J., López-Urrea, R., Jovanovic, N., 2021a.
882 Updates and advances to the FAO56 crop water requirements method. *Agric. Water*
883 *Manag.* 248. <https://doi.org/10.1016/j.agwat.2020.106697>

884 Pereira, L.S., Paredes, P., Hunsaker, D.J., López-Urrea, R., Mohammadi Shad, Z., 2021b.
885 Standard single and basal crop coefficients for field crops. Updates and advances to
886 the FAO56 crop water requirements method. *Agric. Water Manag.* 243, 106466.
887 <https://doi.org/10.1016/j.agwat.2020.106466>

888 Pereira, L.S., Paredes, P., Jovanovic, N., 2020. Soil water balance models for determining
889 crop water and irrigation requirements and irrigation scheduling focusing on the
890 FAO56 method and the dual Kc approach. *Agric. Water Manag.* 241, 106357.
891 <https://doi.org/10.1016/j.agwat.2020.106357>

892 Piccinni, G., Ko, J., Marek, T., Leskovar, D., 2009. Crop coefficients specific to multiple
893 phenological stages for evapotranspiration-based irrigation management of onion
894 and spinach. *HortScience* 44, 421–425.

895 Pohanková, E., Hlavinka, P., Orság, M., Takáč, J., Kersebaum, K.C., Gobin, A., Trnka,
896 M., 2018. Estimating the water use efficiency of spring barley using crop models. *J.*
897 *Agric. Sci.* 156, 628–644. <https://doi.org/10.1017/S0021859618000060>

898 Raes, D., Steduto, P., Hsiao, C., Fereres, E., 2018. Chapter 3. Calculation procedures.

899 Raes, D., Steduto, P., Hsiao, T., Fereres, E., 2017. AquaCrop Plug-in program (Version
900 6.0).

901 Ritchie, J., Godwin, D., Otter-Nacke, S., 1985. CERES-Wheat: A Simulation Model of
902 Wheat Growth and Development, Texas A.&M Univ. press.

903 Ruiz-Corral, J., Flores-López, H., Ramírez-Díaz, J., González-Eguiarte, D., 2002.
904 Cardinal temperatures and length of maturation cycle of maize hybrid H-311 under

- 905 rainfed conditions. *Agrociencia* 36, 569–577.
- 906 Sadras, V.O., Cassman, K.G.G., Grassini, P., Hall, A.J., Bastiaanssen, W.G.M., Laborte,
907 A.G., Milne, A.E., Sileshi, G., Steduto, P., 2015. Yield gap analysis of field crops,
908 Methods and case studies, FAO Water Reports.
- 909 Sánchez-Virosta, A., Lélis, B.C., Pardo, J.J., Martínez-Romero, A., Sánchez-Gómez, D.,
910 Domínguez, A., 2020. Functional response of garlic to optimized regulated deficit
911 irrigation (ORDI) across crop stages and years: Is physiological performance
912 impaired at the most sensitive stages to water deficit? *Agric. Water Manag.* 228, 1–
913 10. <https://doi.org/10.1016/j.agwat.2019.105886>
- 914 Saseendran, S.A., Ahuja, L.R., Ma, L., Trout, T.J., McMaster, G.S., Nielsen, D.C., Ham,
915 J.M., Andales, A.A., Halvorson, A.D., Chávez, J.L., Fang, Q.X., 2015. Developing
916 and normalizing average corn crop water production functions across years and
917 locations using a system model. *Agric. Water Manag.* 157, 65–77.
918 <https://doi.org/10.1016/j.agwat.2014.09.002>
- 919 Schütze, N., De Paly, M., Shamir, U., 2012. Novel simulation-based algorithms for
920 optimal open-loop and closed-loop scheduling of deficit irrigation systems. *J.*
921 *Hydroinformatics* 14, 136–151. <https://doi.org/10.2166/hydro.2011.073>
- 922 Sevacherian, V., Stern, V., Mueller, A., 1977. Heat accumulation for timing Lygus
923 control measures in a safflower-cotton complex. *J. Econ. Entomol.* 70, 399–402.
- 924 SIAR-CLM, 2014. Irrigation Advisory Service of Castilla-La Mancha. Castilla-La
925 Mancha University. Castilla-La Mancha Government. [WWW Document]. URL
926 <http://crea.uclm.es/siar/> (accessed 3.20.15).
- 927 Steduto, P., Hsiao, T., Fereres, E., Raes, D., 2012. Crop Yield Response to Water. FAO
928 Irrigation and Drainage Paper 66, Rome, Italy.
- 929 Steduto, P., Hsiao, T.C., Fereres, E., 2007. On the conservative behavior of biomass water
930 productivity. *Irrig. Sci.* 25, 189–207. <https://doi.org/10.1007/s00271-007-0064-1>
- 931 Steduto, P., Hsiao, T.C., Raes, D., Fereres, E., 2009. Aquacrop-the FAO crop model to
932 simulate yield response to water: I. concepts and underlying principles. *Agron. J.*
933 101, 426–437. <https://doi.org/10.2134/agronj2008.0139s>
- 934 Stewart, J., Hagan, R., 1973. Functions to predict effects of crop water deficits. *J. Irrig.*
935 *Drain. Div.* 99, 421–439.
- 936 Stöckle, C.O., Kemanian, A.R., Nelson, R.L., Adam, J.C., Sommer, R., Carlson, B., 2014.
937 CropSyst model evolution: From field to regional to global scales and from research
938 to decision support systems. *Environ. Model. Softw.* 62, 361–369.
939 <https://doi.org/10.1016/j.envsoft.2014.09.006>
- 940 Tanner, C., Siinclair, T., 1983. Efficient water use in crop production: Research or re-
941 search?, in: Taylor, H., Jordan, W., Sinclair, T. (Eds.), *Limitations to Efficient Water*
942 *Use in Crop Production*. American Society of Agronomy, Madison, WI, pp. 1–27.
- 943 Trout, T.J., DeJonge, K.C., 2017. Water productivity of maize in the US high plains. *Irrig.*
944 *Sci.* 35, 251–266. <https://doi.org/10.1007/s00271-017-0540-1>
- 945 Ugarte, C., Calderini, D.F., Slafer, G.A., 2007. Grain weight and grain number
946 responsiveness to pre-anthesis temperature in wheat, barley and triticale. *F. Crop.*
947 *Res.* 100, 240–248. <https://doi.org/10.1016/j.fcr.2006.07.010>
- 948 Vanuytrecht, E., Raes, D., Steduto, P., Hsiao, T.C., Fereres, E., Heng, L.K., Garcia Vila,

949 M., Mejias Moreno, P., 2014. AquaCrop: FAO's crop water productivity and yield
950 response model. *Environ. Model. Softw.* 62, 351–360.
951 <https://doi.org/10.1016/j.envsoft.2014.08.005>

952 Willmott, C.J., 1982. Some comments on the evaluation of model performance. *Bull. -*
953 *Am. Meteorol. Soc.* 63, 1309–1313. [https://doi.org/10.1175/1520-](https://doi.org/10.1175/1520-0477(1982)063<1309:SCOTEO>2.0.CO;2)
954 [0477\(1982\)063<1309:SCOTEO>2.0.CO;2](https://doi.org/10.1175/1520-0477(1982)063<1309:SCOTEO>2.0.CO;2)

955

956

957

958 **SUPPLEMENTAL MATERIAL**

959 Table A1. Duration of barley phenological stages in Castilla-La Mancha (days) according
 960 to development stages for MOPECO and AquaCrop models.

	MOPECO								AquaCrop			Dates		
	K _c (I)	K _c (II)	K _c (III)	K _c (IV)	K _y (i)	K _y (ii)	K _y (iii)	K _y (iv)	CnDv	MSsn	LSsn	Total	First day after sowing	Maturity
Start	0	21	39	83	0	37	71	85	0	39	71	00		
End	21	39	83	89	37	71	85	89	39	71	89	89		
	Duration (days)													
2002a	49	60	22	17	102	22	11	13	109	15	24	148	31st Jan.	27th Jun.
2002b	55	54	26	24	94	34	14	17	109	19	31	159	10th Jan.	17th Jun.
2002c	76	40	25	23	110	25	11	18	116	19	29	164	5th Jan.	17th Jun.
2003b	66	47	21	17	103	24	11	13	113	14	24	151	14th Jan.	13th Jun.
2003b	76	43	22	20	113	23	11	14	119	17	25	161	2nd Jan.	11th Jun.
2003d	74	43	23	18	110	23	10	15	117	16	25	158	2nd Jan.	8th Jun.
2003c	73	45	24	19	114	22	10	15	118	18	25	161	10th Jan.	19th Jun.
2004a	51	64	23	18	108	24	11	13	115	17	24	156	30th Jan.	4th Jul.
2004c	49	62	32	17	100	35	14	11	111	24	25	160	12th Jan.	20th Jun.
2004c	56	58	24	16	108	23	11	12	114	17	23	154	17th Jan.	19th Jun.
2005b	59	41	24	19	95	23	11	14	100	18	25	143	21st Jan.	12th Jun.
2005e	68	47	23	17	106	25	11	13	115	16	24	155	7th Jan.	10th Jun.
2005c	67	38	22	23	98	23	13	16	105	16	29	150	15th Jan.	13th Jun.
2005f	63	43	22	19	99	22	12	14	106	15	26	147	15th Jan.	10th Jun.
2007c	45	47	23	21	84	25	12	15	92	17	27	136	7th Feb.	22nd Jun.
2008c	46	52	26	23	85	34	12	16	98	21	28	147	24th Jan.	19th Jun.
2009g	48	50	20	18	91	20	12	13	98	13	25	136	1st Feb.	16th Jun.
2009h	39	55	21	20	82	26	15	12	94	14	27	135	5th Feb.	19th Jun.
2009i	39	53	23	19	87	22	12	13	92	17	25	134	6th Feb.	19th Jun.
2009c	55	55	24	18	103	24	12	13	110	17	25	152	19th Jan.	19th Jun.
2010h	67	44	26	22	101	26	16	16	111	16	32	159	11th Jan.	18th Jun.
2010a	69	51	21	21	113	22	11	16	120	15	27	162	17th Jan.	27th Jun.
2010g	52	53	21	17	99	22	10	12	105	16	22	143	2nd Feb.	24th Jun.
2010j	52	42	22	24	87	24	11	18	94	17	29	140	5th Feb.	24th Jun.
2010k	45	41	31	20	81	30	13	13	86	25	26	137	5th Feb.	19th Jun.
2011a	61	37	27	26	87	32	17	15	98	21	32	151	21st Jan.	20th Jun.
2012a	61	42	24	20	93	26	13	15	103	16	28	147	30th Jan.	25th Jun.
2013a	62	40	29	21	92	32	13	15	102	22	28	152	30th Jan.	30th Jun.

961 where K_c (I): Initial; K_c (II): Crop development; K_c (III): Mid-season; K_c (IV): Late season; K_y (i):
 962 Vegetative period; K_y (ii): Flowering period; K_y (iii): Yield formation; K_y (iv): Ripening; CnDv: canopy
 963 development; MSsn: mid-season; LSsn: late season; 00: First day after sowing; 21: Beginning of tillering;
 964 first tiller detectable; 37: Flag leaf just visible, still rolled; 39: Flag leaf stage: flag leaf fully unrolled, ligule
 965 just visible; 71: Watery ripe: first grains have reached half their final size; 83: Early dough; 85: Soft dough:
 966 grain content soft but dry. Fingernail impression not held; 89: Fully ripe: grain hard, difficult to divide with
 967 thumbnail. Irrigable area: a: Las Tiesas; b: Manzanares; c: El Sanchón; d: Daimiel; e: Ciudad Real; f:
 968 Magán; g: Almansa; h: Montiel; i: Hellín; j: Ontur; k: El Pedernoso

969

970

971

972

973

974 Table A2. Duration of barley phenological stages in Castilla-La Mancha (GDD)
 975 according to development stages for MOPECO and AquaCrop models.

Year	MOPECO								AquaCrop		
	K _c (I)	K _c (II)	K _c (III)	K _c (IV)	K _y (i)	K _y (ii)	K _y (iii)	K _y (iv)	CnDv	MSsn	LSsn
2002a	296	892	1214	1561	793	1125	1288	1561	875	1103	1509
2002b	256	740	1051	1473	559	952	1165	1473	710	918	1407
2002c	384	754	1031	1400	662	951	1101	1400	716	912	1351
2003b	334	793	1117	1460	666	1007	1190	1460	763	971	1391
2003b	357	751	1076	1448	677	988	1167	1448	722	954	1383
2003d	383	794	1149	1490	706	1019	1206	1490	772	993	1438
2003c	350	771	1134	1521	732	1042	1208	1521	726	995	1451
2004a	297	835	1227	1599	748	1120	1318	1599	812	1088	1529
2004c	232	665	1054	1377	551	918	1172	1377	626	878	1321
2004c	278	705	1031	1336	657	909	1111	1336	666	870	1281
2005b	228	660	1009	1388	582	912	1109	1388	602	853	1294
2005e	216	729	1062	1405	603	951	1143	1405	650	874	1296
2005c	290	672	1000	1438	577	914	1126	1438	598	839	1345
2005f	259	754	1093	1488	647	986	1193	1488	698	927	1395
2007c	295	693	1011	1377	610	936	1111	1377	683	924	1359
2008c	253	705	1033	1374	564	972	1119	1374	683	949	1344
2009g	284	755	1077	1412	661	965	1171	1412	743	948	1377
2009h	222	695	1019	1402	551	905	1153	1402	684	890	1364
2009i	272	798	1175	1550	731	1073	1289	1550	791	1062	1503
2009c	297	793	1178	1524	691	1055	1266	1524	770	1030	1471
2010h	285	734	1021	1361	594	864	1124	1361	718	848	1337
2010a	334	814	1165	1492	757	1041	1241	1492	795	1018	1449
2010g	283	789	1137	1398	733	1038	1218	1398	769	1010	1360
2010j	328	776	1087	1506	708	1000	1212	1506	770	993	1486
2010k	226	660	1053	1363	578	950	1195	1363	648	937	1340
2011a	276	687	1062	1513	567	961	1232	1513	661	935	1465
2012a	283	704	1116	1496	563	962	1206	1496	655	905	1407
2013a	327	728	1059	1437	600	960	1174	1437	705	938	1397
Average	290	744	1087	1450	645	981	1186	1450	715	949	1395
SD	46	57	64	69	73	64	59	69	66	71	68
CV (%)	16	8	6	5	11	7	5	5	9	7	5

976

977

978

979

980

981

982

983

984

985

986 Table A3. Statistical indicators of the crop-water and IWP-water production functions for
 987 different irrigation strategies.

PF	IS	SE	R ²	p-value	Parameters	Polynomial model values
Y-GIWD	IS1	393.0	97.3	**	a	2634.020**
					b	28.049**
					c	-0.021**
	IS2	381.1	97.7	**	a	2763.490**
					b	28.887**
					c	-0.014*
	IS3	851.3	92.7	**	a	1708.150*
					b	36.778**
					c	-0.029*
	IS4	724.4	94.4	**	a	2264.760**
					b	25.438**
					c	0.003 ^{ns}
	ORDI	224.1	99.2	**	a	2711.230**
					b	39.640**
					c	-0.035**
ORDIL	177.6	99.7	**	a	2772.720**	
				b	39.262**	
				c	-0.033**	
IWP-GIWD	IS1	0.19	84.6	**	a	5.06**
					b	-0.01**
	IS2	0.06	90.0	**	a	6.46**
					b	-0.02**
	IS3	0.10	82.1	**	a	4.74**
					b	-0.01**
	IS4	0.07	48.7	**	a	4.12**
					b	-0.0022*
	ORDI	0.02	98.0	**	a	6.50**
					b	-0.01**
	ORDIL	0.01	99.8	**	a	6.22**
					b	-0.01**

988 PF: production function; Y: yield; GIWD: gross irrigation water depth; IS: irrigation strategy; Aq:
 989 AquaCrop; MOP: MOPECO; SE: standard error of the model (kg ha⁻¹); R²: coefficient of determination; p-
 990 value: model's significance level; ns: not significant, p>0.05; *: significant, 0.01≤p<0.05; **: highly
 991 significant, p<0.01